INSTITUT D'AERONOMIE SPATIALE DE BELGIQUE

3 - Avenue Circulaire
B - 1180 BRUXELLES

AERONOMICA ACTA

A - N° 160 - 1976

ABSORPTION AND PHOTODISSOCIATION IN THE SCHUMANN-RUNGE BANDS OF MOLECULAR OXYGEN IN THE TERRESTRIAL ATMOSPHERE

by

G. KOCKARTS

BELGISCH INSTITUUT VOOR RUIMTE-AERONOMIE

3 - Ringlaan
B - 1180 BRUSSEL

FOREWORD

The paper "Absorption and photodissociation in the Schumann-Runge bands of molecular oxygen in the terrestrial atmosphere" will be published in Planetary and Space Sciences, **24**, 1976.

AVANT-PROPOS

L'article "Absorption and photodissociation in the Schumann-Runge bands of molecular oxygen in the terrestrial atmosphere" sera publié dans Planetary and Space Sciences, **24**, 1976.

VOORWOORD

De tekst "Absorption and photodissociation in the Schumann-Runge bands of molecular oxygen in the terrestrial atmosphere" zal in Planetary and Space Sciences, **24**, 1976 uitgegeven worden.

VORWORT

Der Text "Absorption and photodissociation in the Schumann-Runge bands of molecular oxygen in the terrestrial atmosphere" wird in Planetary and Space Sciences, **24**, 1976 herausgegeben werden.

ABSORPTION AND PHOTODISSOCIATION IN THE SCHUMANN-RUNGE BANDS OF MOLECULAR OXYGEN IN THE TERRESTRIAL ATMOSPHERE

by

G. KOCKARTS

Abstract

The penetration in the terrestrial atmosphere of solar radiation corresponding to the spectral range of the Schumann-Runge bands of molecular oxygen is analyzed between 1750 Å and 2050 Å. The variation of the absorption cross section with temperature is taken into account and it is shown that average O_2 absorption cross sections cannot lead to correct photodissociation coefficients. Reduction factors are defined in order to simplify the computation of the molecular oxygen photodissociation and to permit a simple determination of the photodissociation coefficients of any minor constituent with smoothly varying absorption cross section. Examples are given for O_2, H_2O, CO_2, N_2O, HNO_3 and H_2O_2. Numerical approximations are developed for three types of spectral subdivisions : Schumann-Runge band intervals, 500 cm^{-1} and 10 Å intervals. The approximations are valid from the lower thermosphere down to the stratosphere and they can be applied for a wide range of atmospheric models and solar zenith distances.

Résumé

La pénétration du rayonnement solaire dans le domaine spectral des bandes de Schumann-Runge de l'oxygène moléculaire est analysée entre 1750 Å et 2050 Å pour les conditions physiques de l'atmosphère terrestre. La variation de la section efficace d'absorption avec la température est prise en compte et on montre que des sections efficaces moyennes ne peuvent pas conduire à des coefficients de photodissociation corrects. Des facteurs de réduction sont définis afin de simplifier le calcul des coefficients de photodissociation de l'oxygène moléculaire et de tout constituant minoritaire dont la section efficace varie uniformément avec la longueur d'onde. Les constituants O_2, H_2O, CO_2, N_2O, HNO_3 et H_2O_2 sont traités à titre d'exemple. Des approximations numériques sont développées pour trois types de subdivisions spectrales, c'est-à-dire les intervalles des bandes de Schumann-Runge ainsi que des intervalles de 500 cm^{-1} et de 10 Å. Les approximations sont valables de la thermosphère inférieure jusque dans la stratosphère. De plus, elles peuvent être appliquées à un large domaine de modèles atmosphériques et pour des distances solaires zénithales inférieures à 75°.

Samenvatting

De indringing van de zonnestraling in het spectraal gebied van de Schumann-Runge banden van moleculaire zuurstof wordt geanalyseerd tussen 1750 Å en 2050 Å voor de fysische voorwaarden van de aardse atmosfeer. De verandering van de werkzame absorptiedoorsnede in functie van de temperatuur wordt in rekening gebracht en men toont aan dat gemiddelde werkzame doorsneden niet kunnen leiden tot juiste fotodissociatiecoefficienten. Reductiefactoren worden gedefinieerd ten einde de berekening van de fotodissociatiecoefficienten van moleculaire zuurstof en van om het even welk minderheidsbestanddeel waarvan de werkzame doorsnede eenvormig verandert met de golflengte te vereenvoudigen. Ten titel van voorbeeld worden de bestanddelen O_2, H_2O, CO_2, N_2O, HNO_3 en H_2O_2 behandeld. Numerieke benaderingen worden ontwikkeld voor drie typen van spectrale onderverdelingen, t.t.z. de intervallen van de Schumann-Runge banden alsook intervallen van 500 cm^{-1} en van 10 Å. De benaderingen zijn geldig van de lage thermosfeer tot de stratosfeer. Wat meer is, ze kunnen toegepast worden bij een brede waaier van atmosferische modellen en voor zenitsafstanden van de zon kleiner dan 75°.

Zusammenfassung

Das Durchdringen der Sonnenstrahlung im Wellenlängegebiet der Schumann-Runge Banden von Molekularsauerstoff wird zwischen 1750 Å und 2050 Å für physikalischen Bedingungen der Erdeatmosphäre analysiert. Die Temperaturvariation des Absorptionwirkungsquerschnittes ist einbegriffen und es wird gezeigt, dass mittlere Querschnitte keine genaue Photodissoziationskoeffizienten geben. Reduktionsfaktoren sind definiert sodass das Rechnen der Photodissoziationskoeffizienten von Molekularsauerstoff und von Minderheitskomponenten, für welche die Querschnitte gleichformig mit der Wellenlänge ändern, einfacher ist. Die Komponenten O_2 H_2O, CO_2, N_2O, HNO_3 und H_2O_2 werden als Beispiele behandelt. Nümerische Näherungen werden für drei Spektralunterabteilungen, nähmlich Schumann-Runge Banden, 500 cm^{-1} und 10 Å, festgestellt. Diese Näherungen sind von der unteren Thermosphäre bis zur Stratosphäre gültig und sie können auf verschiedene atmosphärische Modellen und Zenitdistanzen angewendet werden.

INTRODUCTION

In the wavelength region between 1750 Å and 2050 Å, the major atmospheric absorption of solar radiation results from the numerous lines of the Schumann-Runge band system ($B^3\Sigma_u^- \leftarrow X^3\Sigma_g^-$) of molecular oxygen. Detailed computations of the penetration of solar radiation through the Schumann-Runge bands (Kockarts, 1971) require the knowledge of high resolution absorption cross sections (Ackerman *et al.*, 1970). This implies that a large amount of cross sections have to be stored in some way, especially since the absorption cross section is temperature dependent. Kockarts (1971) computed the absorption cross section at every 0.5 cm^{-1} in the Schumann-Runge bands and used 17 sets of 16000 absorptions cross sections corresponding to temperatures which range from 160 K to 320 K with 10 K interval.

Several attempts have been made to reduce the computer time and cost implied by such a procedure (Brinkmann, 1969; 1971; Anderson, 1971; Hudson and Mahle, 1972; Whitten and Turco, 1974; Fang *et al.*, 1974; Park, 1974). Any approximation should, however, be designed for a specific purpose. Two major problems are actually of practical significance : the photodissociation of O_2 itself and the absorption by O_2 which influences the photodissociation of several minor atmospheric constituents. These two question are discussed in this paper and approximate expressions are given to compute the solar penetration in the mesosphere and stratosphere, the photodissociation coefficients of O_2 and of the minor constituents which can be dissociated within the spectral range of the Schumann-Runge bands.

2. ABSORPTION CROSS SECTIONS AND SOLAR FLUXES

The major difficulty for using the absorption cross sections of molecular oxygen in the Schumann-Runge bands results from their large variation with wavelength and with temperature. The absorption cross sections discussed by Ackerman *et al.* (1970) change from 10^{-18} cm^2 at roughly 1750 Å to 10^{-23} cm^2 at 2050 Å. Within a specific band, varia-

tions of 3 orders of magnitude are very common. As a consequence the optical depth is characterized by large variations over rather narrow wavelength intervals (Kockarts, 1971).

The molecular oxygen absorption cross sections in the Schumann-Runge bands essentially depend on various molecular parameters and on one atmospheric parameter, namely the temperature.

The molecular parameters are the line positions, the line widths and the band integrated absorption coefficients which are related to the band oscillator strengths. In the present paper, the molecular parameters are identical to the values used previously (Ackerman *et al.* 1970; Biaumé, 1972a, b; Kockarts, 1972). The band oscillator strengths adopted by Biaumé (1972b) are in very good agreement with the values computed by Allison *et al.* (1971) and they also agree closely with the electron impact values obtained by Huebner *et al.* (1975) between the vibrational levels $v' = 4$ and $v' = 11$. In their computation of the O_2 photodissociation coefficient, Hudson and Mahle (1972) adopted similar oscillator strengths except for $v' = 13$, 14 and 17 to 19. It should be noted that for $v' = 13$ and 14 there is also a very large discrepancy between the line widths of Hudson and Mahle (1972) and the values used by Ackerman *et al.* (1970). The important problem of line width determination has been analyzed theoretically by Julienne and Krauss (1975). They showed that a rather large discrepancy exists between theoretical and experimental line widths for $v' = 5$ to 11 and they suggest that the difference could be due to line blending. Apparently, more experimental and theoretical work is needed before this question can be solved. The agreement between the O_2 photodissociation coefficient (Kockarts 1971) computed with the line widths of Ackerman *et al.* (1970) and the values obtained by Hudson and Mahle (1972) with their line widths is, however, satisfactory. Furthermore, the water vapor photodissociation coefficient obtained by Fang *et al.* (1974) with the line widths of Hudson and Mahle (1972) agrees also with the values computed by Kockarts (1971). It seems, therefore, that the line width problem is not so crucial when photodissociation coefficients of O_2 and other minor constituents are computed over the whole Schumann-Runge bands. This is, however, not correct for a computation at a specific wavelength. Finally, it is worthwhile to mention that more precise molecular constants for

the Schumann-Runge system have been obtained by Creek and Nicholls (1975). These constants can be used to compute line positions. Ackerman *et al.* (1970) used however experimental line positions for the v" = 0 progression and molecular constants where only used to compute the line positions for the v" = 1 bands. A calculation made with the new values of Creek and Nicholls (1975) indicates that up to the lines 13 R and 13 P of the v" = 1 bands the agreement is very good, of the order of 0.1 cm^{-1}. For higher quantum numbers in the R and P branches, larger differences occur. This implies again that with these new molecular constants, changes can occur at specific wavelengths within a band. Since the purpose of the present paper is to provide *average* photodissociation coefficients, the previous molecular parameters given by Ackerman *et al.* (1970) are not modified in the following computations. When all the molecular parameters discussed previously are known with better accuracy, it will necessary to recompute the detailed absorption cross sections. This is particularly true for the analysis of future in situ observations made with a resolution better than 0.5 cm^{-1} i.e. approximately 0.02 A in the wavelength range of the Schumann–Runge bands system.

Since the temperature in the homosphere can vary between 160 K and 300 K at different levels, the influence on the O_2 absorption cross section will be discussed in this temperature range. With the expressions used by Ackerman *et al.* (1970) and by Kockarts (1972), it can be shown that the ratio $\sigma(T_1)/\sigma(T_2)$ of the absorption cross for the temperatures T_1 and T_2 is given by

$$\sigma(T_1)/\sigma(T_2) = \frac{T_2 F(T_1,v'')}{T_1 F(T_2,v'')} \quad \exp\left[-a\left(\frac{1}{T_1} - \frac{1}{T_2}\right)\right] \qquad (1)$$

where $F(T_1,v'')$ and $F(T_2,v'')$ are respectively the relative numbers of molecules in the vibrational level v" for T_1 and T_2 (Herzberg, 1950). The quantity a is given by

$$a = (hc/k)\, B_{v''}\, N''(N'' + 1) \qquad (2)$$

where h is Planck's constant, c is the speed of light, k is Boltzmann's constant, $B_{v''}$ is the rotational constant of the vibrational level v" and N" is the rotational quantum number of

the v" levels which takes the values 1, 3, 5, 7 ... Expression (1) is only rigorously valid for the absorption cross section resulting from a single line and it reflects the variation of the relative intensity of the various lines in a specific band. For the lowest vibrational level v" = 0, $F(T_1,0) = F(T_2,0) = 1$. Taking $B_o = 1.43771\ cm^{-1}$ (Creek and Nicholls, 1975) and introducing the other numerical constants in (2), expression (1) leads to the ratio

$$\sigma(T_1)/\sigma(T_2) = (T_2/T_1) \exp [- 1.955\ N"(N" + 1)] \qquad (3)$$

for the cross sections in a P or R branch of the v" = 0 bands. With $T_1 = 150$ K and $T_2 = 300$ K, expression (3) shows that $\sigma(150)$ is greater than $\sigma(300)$ for N" < 11 and that the inverse relation occurs for N" > 11. Therefore, the absorption cross section is a decreasing function of the temperature near the band heads and an increasing function of the temperature from a certain value of N" which depends on the temperature. The real behavior of the cross section is a little more complicated since at a specific wavelength the cross section results from the overlapping of several lines. Furthermore the v" = 1 progression cannot be neglected for temperatures above 200 K. Fig. 1 shows variations of the absorption cross section as a function of temperature at various wavelengths in the P branch of the 4-0 band. The characteristics deduced from expression (3) are found in Figure 1; for example, the cross section becomes an increasing function of temperature at the 11 P line and the cross section increases by a factor of 5 between 160 K and 300 K for the 19 P line. Since there is a reversal in the temperature dependence within each band, it is instructive to examine the behavior of the mean absorption cross section computed for each band. These mean absorption cross sections for two extreme temperatures, namely 160 K and 300 K are given in Figure 2 which shows that there is no strong temperature dependence. The first impression is, therefore, that such values are appropriate for the computation of solar radiation absorption and of photodissociation coefficients. However, it will be shown in the next section which type of error is introduced when such mean absorption cross sections are used. The errors which arise from the use of mean absorption cross sections are actually a consequence of very large standard deviations which characterize such mean absorption cross sections. As an example, the mean absorption cross section for 250 K in the 9-0 band is $2.0 \times 10^{-20}\ cm^2$ with a standard deviation of $5.4 \times 10^{-20}\ cm^2$. It appears, therefore, that

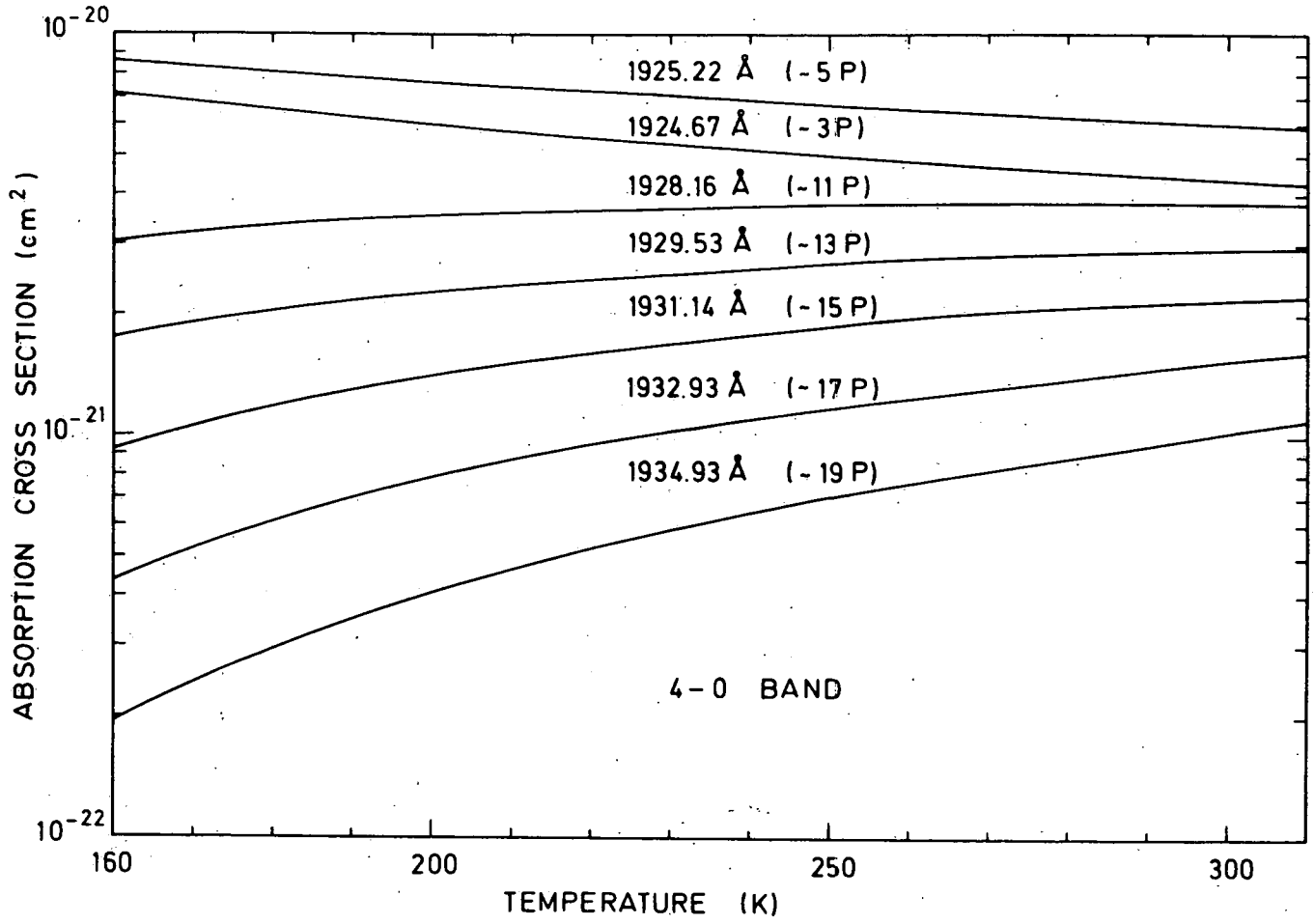

Fig. 1.- Absorption cross sections at specific wavelengths in the 4-0 band of the O_2 Schumann-Runge system as a function of temperature. The wavelengths correspond to various lines in the P branch.

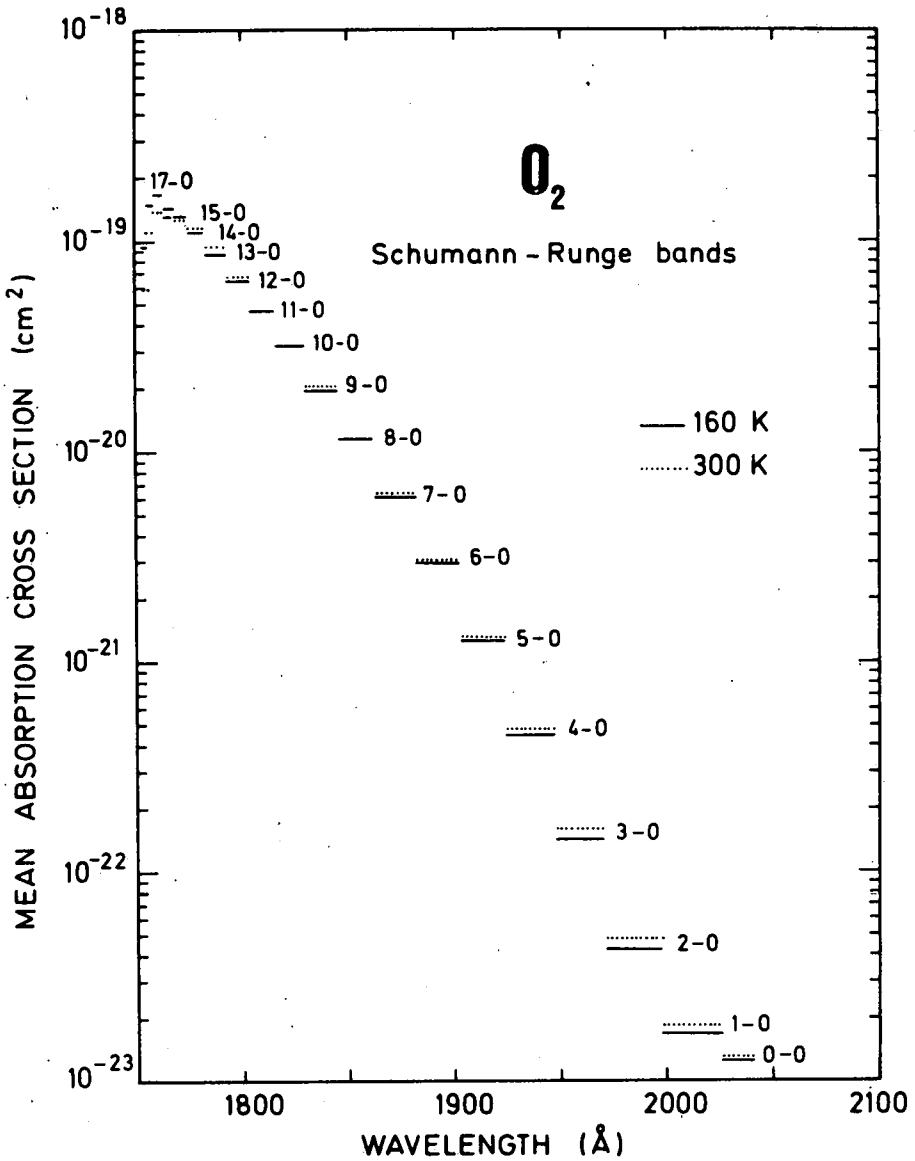

Fig. 2.- Mean absorption cross sections in the various bands of the O_2 Schumann-Runge system for two extreme stratospheric and mesospheric temperatures, namely 160 K and 300 K.

TABLE I.- Average solar fluxes and average absorption cross sections of minor constituents in the spectral range of the Schumann-Runge bands of O_2.

Bands (v'-v")	Wavenumbers (cm^{-1})	Wavelengths (Å)	Photons ($cm^{-2} s^{-1} \Delta\lambda^{-1}$)	Absorption cross sections (cm^{-2})				
				H_2O	CO_2	N_2O	H_2O_2	HNO_3
19 - 0	57030.5	1753.45	1.50×10^{10}	2.40×10^{-18}	5.18×10^{-21}	1.18×10^{-19}	—	—
18 - 0	56954.5	1755.79	2.10	2.35	4.52	1.19	—	—
17 - 0	56852.5	1758.94	2.81	2.25	4.51	1.20	—	—
16 - 0	56719.5	1763.06	3.84	2.20	3.81	1.21	—	—
15 - 0	56550.5	1768.33	6.40	1.95	3.33	1.23	—	—
14 - 0	56340.5	1774.92	8.38	1.70	2.74	1.30	—	—
13 - 0	56085.5	1782.99	1.26×10^{11}	1.45	1.78	1.32	—	—
12 - 0	55784.5	1792.61	1.56	8.10×10^{-19}	1.48	1.37	—	—
11 - 0	55439.0	1803.78	2.08	4.20	1.10	1.40	1.60×10^{-18}	—
10 - 0	55051.0	1816.50	2.91	1.90	7.91×10^{-22}	1.40	1.45	—
9 - 0	54622.0	1830.76	3.13	7.40×10^{-20}	5.19	1.35	1.38	—
8 - 0	54156.5	1846.50	3.42	3.80	3.00	1.30	1.02	—
7 - 0	53656.5	1863.71	4.98	1.80	1.59	1.22	8.80×10^{-19}	1.60×10^{-17}
6 - 0	53123.0	1882.42	6.02	7.20×10^{-21}	8.41×10^{-23}	1.12	8.00	1.50
5 - 0	52561.5	1902.53	7.58	2.90	4.76	1.05	7.00	1.47
4 - 0	51970.0	1924.19	8.15	9.80×10^{-22}	2.45	8.80×10^{-20}	6.20	1.25
3 - 0	51352.5	1947.32	1.22×10^{12}	3.70	1.32	7.00	5.80	9.20×10^{-18}
2 - 0	50711.0	1971.96	1.38	1.25	3.97×10^{-24}	4.80	5.30	6.70
1 - 0	50046.0	1998.16	1.79	3.70×10^{-23}	1.44	3.40	4.95	4.65
0 - 0	49358.0	2026.01	1.09	—	8.62×10^{-25}	2.45	4.70	3.30

the temperature dependence of the absorption cross section should be included in any detailed computations, although Park (1974) used only absorption cross sections at 250 K for computing O_2 and H_2O photodissociation coefficients and neglected the v" = 1 progression.

High resolution solar spectra are now becoming available in the Schumann-Runge spectral region. Recently, Samain and Simon (1976) used a solar spectrum obtained by Samain *et al.* (1975) at the center of the solar disk with a resolution of 0.4 Å, to determine the whole solar disk flux between 1600 Å and 2100 Å using center to limb darkening curves. The spectral region of the Schumann-Runge bands is illustrated by Figure 3. Even if the structure is rather well known, errors in the absolute calibration of the measured solar fluxes are, however, not excluded. The average error is estimated to be less than ± 25 % (Samain *et al.* 1975). The spectrum of Figure 3 has been interpolated every 0.5 cm^{-1} when detailed computations are required. The origins of the bands in the Schumann-Runge system are also indicated on Figure 3 by the upper vibrational level v' in order to show where the fine structure of the solar spectrum could play a role.

For the calculation of photodissociation coefficients of minor constituents with smoothly varying cross sections, we can use, however, the band average fluxes as given in Table I without making an important error. The solar fluxes quoted in Table I are given as an example which should allow future comparisons with other values. It is, however important to note that the approximations developped in the present paper are independent of the exact values of the solar fluxes.

The wavenumbers of the band origins, rounded off to half a wavenumber, are also given in Table I, as well as the average absorption cross sections for the minor constituents which will be considered in the next section. The H_2O and H_2O_2 absorption cross sections are obtained by interpolation from the values used by Nicolet (1971). The carbon dioxide absorption cross sections are from Shemansky (1972). The N_2O values result from interpolation in the values adopted by Nicolet and Peetermans (1972) whereas the nitric acid data are taken from Biaumé (1973).

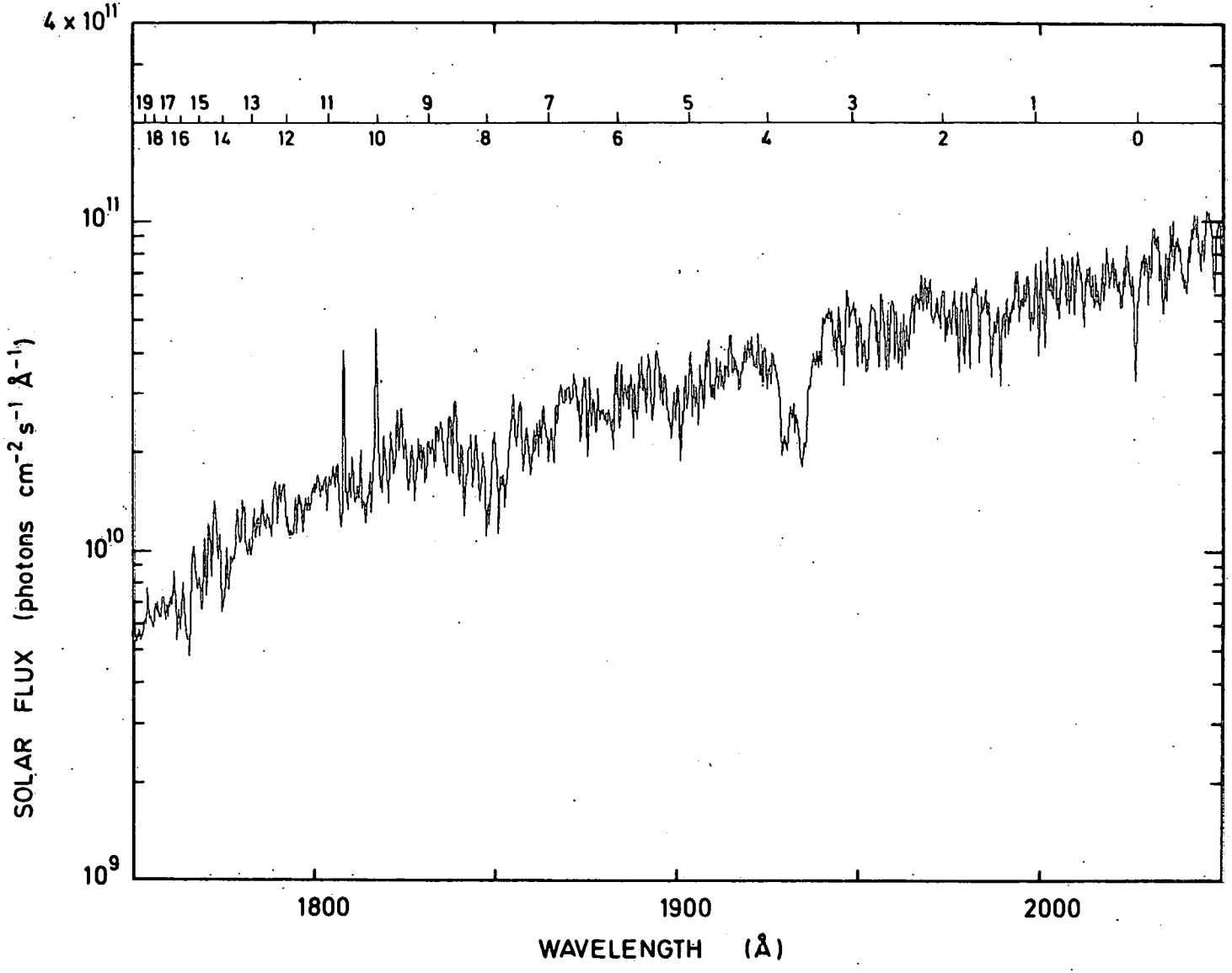

Fig. 3.- Solar flux in the O_2 Schumann-Runge spectral region as determined by Samain and Simon (1976). Band origins are indicated by the upper vibrational quantum number.

3. REDUCTION FACTORS AND PHOTODISSOCIATION COEFFICIENTS

In the lower thermosphere and mesosphere, molecular oxygen is certainly the principal atmospheric constituent absorbing the solar radiation in the Schumann-Runge spectral region. In the stratosphere, however, the absorption by ozone cannot be neglected. The expressions presented in this section consider only the absorption by molecular oxygen and it will be indicated how the ozone effect can be taken into account. Such a procedure is adopted to simplify the discussion pertinent to the molecular oxygen absorption.

The Schumann-Runge system is first divided in 20 wavelengths intervals, from (19-0) to (0-0), each one commencing at a band origin and the last one ending at 49000 cm^{-1}, i.e. 2040.8 Å. Furthermore, each of the 20 band intervals b is divided in a certain number n_b of subintervals where the O_2 absorption cross section σ_{ib} is computed every 0.5 cm^{-1}. If $\phi_{ib}(\infty)$ represents the solar flux available at the top of the atmosphere in a subinterval, the solar flux $\phi_b(z)$ reaching the height z in a band b is given by

$$\phi_b(z) = \sum_{i=1}^{n_b} \phi_{ib}(\infty) \exp(-\tau_{ib}) \tag{4}$$

The optical depth τ_{ib} is given by,

$$\tau_{ib} = \int_z^\infty \sigma_{ib}\, n(O_2)\, ds \tag{5}$$

where $n(O_2)$ is the molecular oxygen concentration and the element ds is taken along the path of the radiation. Since the absorption cross section is temperature dependent, σ_{ib} must be kept under the integral sign, contrary to the formulation of Park (1974). The photodissociation coefficient of a minor constituent M for which the photodissociation cross section $\sigma_b(M)$ can be considered as constant over a band interval is then simply

$$J_b(M) = \sigma_b(M)\, \phi_b(z) \tag{6}$$

where $\phi_b(z)$ is given by equation (4).

The photodissociation coefficient of molecular oxygen $J_b(O_2)$ in one band b of the Schumann-Runge system can be written

$$J_b(O_2) = \sum_{i=1}^{n_b} \epsilon_b \sigma_{ib} \phi_{ib}(\infty) e^{-\tau_{ib}} \qquad (7)$$

In expression (7), ϵ_b represents the predissociation probability in a band b. This probability is not yet known and it will be assumed here that ϵ_b is equal to unity. The difference of a predissociation effect starting at v' = 0 or at v' > 3 has been considered by Kockarts (1971).

From expressions (4), (6) and (7), it appears that no further significant algebraic manipulations can be made, if the fine structure of the solar spectrum is to be taken into account. In order to show the relative importance of the various bands as a function of height, Figure 4 gives different fractions of the O_2 Schumann-Runge photodissociation coefficient computed with the solar fluxes corresponding to the detailed solar spectrum of Samain and Simon (1976). The absorption and photodissociation in the O_2 Herzberg continuum for $\lambda < 2424$ Å can lead to a significant contribution mainly for wavelengths above 1900 Å. Therefore, the absorption cross sections deduced by Jarmain and Nicholls (1967) for the Herzberg continuum are added to the Schumann-Runge bands absorption cross sections over the whole spectral range. Constant values are adopted for spectral intervals of 200 cm^{-1} (Kockarts, 1972). The four curves correspond respectively to the following spectral intervals : 1753.46 Å - 1774.92 Å for bands 19-0 to 15-0, 1774.92 Å - 1830.76 Å for bands 14-0 to 10-0, 1830.76 Å - 1924.19 Å for bands 9-0 to 5-0, and 1924.19 Å - 2040.82 Å for bands 4-0 to 0-0. The computation is made for an overhead sun with the temperature profile and the molecular oxygen concentration from the US Standard atmosphere 1962 (COESA, 1962). It can be seen that the effect of the short wavelength spectral range is almost entirely negligible below the mesopause. In the lower thermosphere the bands 14-0 to 10-0 give the major contribution to the dissociation of the Schumann-Runge band system. The bands 9-0 to 5-0 have their dominant effect in the mesosphere, whereas the bands 4-0 to 0-0 play the major role in the stratosphere. The v'' = 1 progression is included in the results shown in Figure 4.

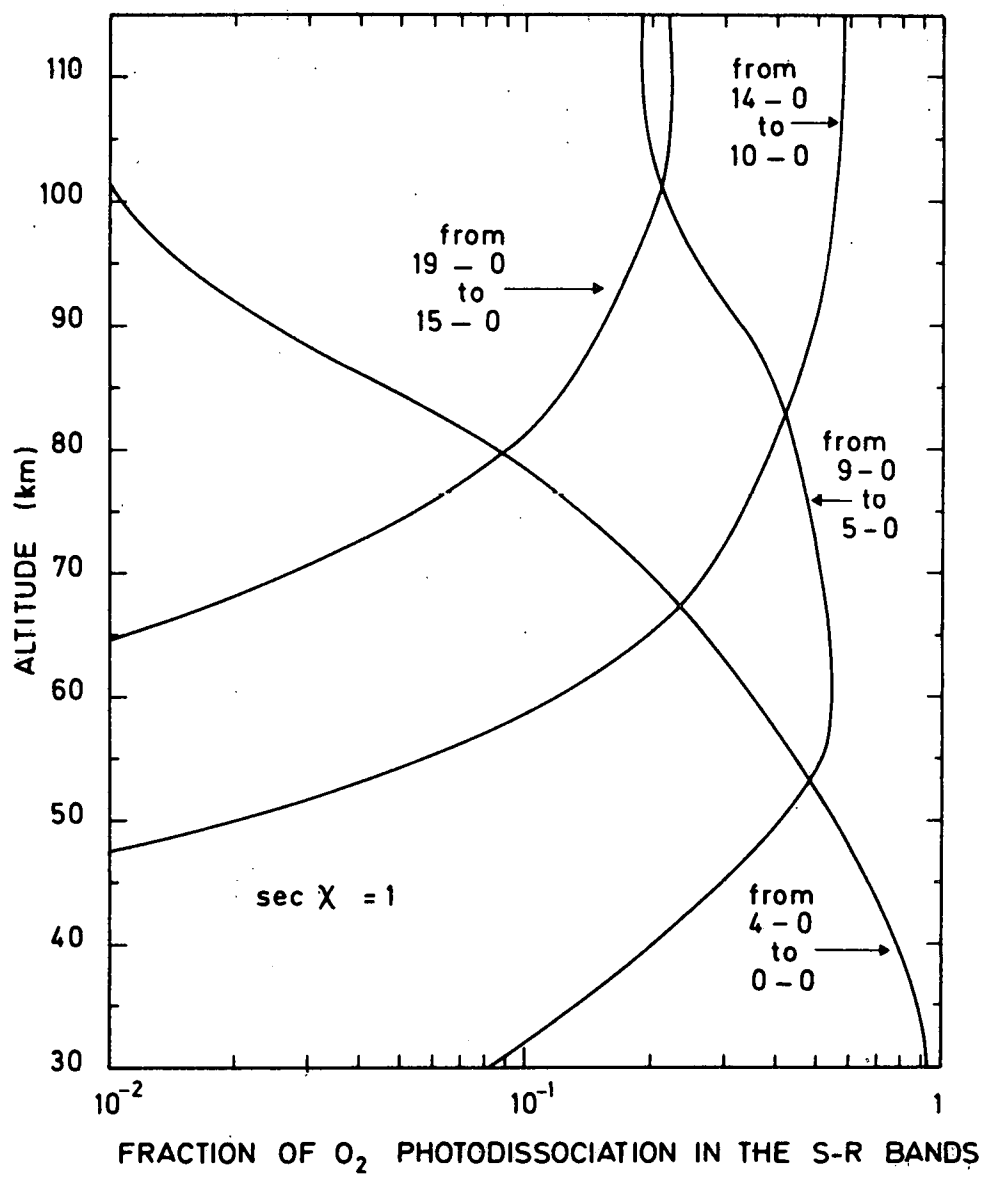

Fig. 4.- Vertical distribution of various fractions of O_2 photodissociation for 4 groups of bands of the Schumann-Runge system : 19-0 to 15-0, 14-0 to 10-0, 9-0 to 5-0 and 4-0 to 0-0. Overhead sun conditions.

A major simplification is possible in expressions (4) and (7) when use in made of a band average solar flux $\phi_b(\infty)$ such that

$$\phi_b(\infty) = \sum_{i=1}^{n_b} \phi_{ib}(\infty) = n_b \, \phi'_{ib}(\infty) \tag{8}$$

When the flux $\phi'_{ib}(\infty)$ defined by (8), is used in equation (4) and (7) instead of $\phi_{ib}(\infty)$ one obtains

$$\phi_b(z) = \phi_b(\infty) \frac{1}{n_b} \sum_{i=1}^{n_b} \exp(-\tau_{ib}) \tag{9}$$

and

$$J_b(O_2) = \phi_b(\infty) \frac{1}{n_b} \sum_{i=1}^{n_b} \epsilon_b \, \sigma_{ib} \exp(-\tau_{ib}) \tag{10}$$

Total photodissociation coefficients computed with equation (10) differ by less than 1% from those obtained with equation (7). Inspection of the solar spectrum (Figure 3) shows, however, that in the 11-0 and 10-0 bands where the two SiII emission lines are observed and in the 4-0 band where the AlI absorption occurs, a detailed computation is preferable when one looks only for specific effects in these spectral intervals.

The reduction factors $R_b(M)$ and $R_b(O_2)$ introduced by Kockarts (1971) are now defined for each band b as

$$R_b(M) = \frac{1}{n_b} \sum_{i=1}^{n_b} \exp(-\tau_{ib}) \tag{11}$$

and

$$R_b(O_2) = \frac{1}{n_b} \sum_{i=1}^{n_b} \epsilon_b \, \sigma_{ib} \exp(-\tau_{ib}) \tag{12}$$

The dimensionless reduction factor $R_b(M)$ is the equivalent of the transmission function used by Fang *et al.* (1974) and $R_b(O_2)$ in cm^2 is equivalent to the expression used by Fang *et al.* (1974) for the computation of the O_2 photodissociation. Similar expressions have also by adopted by Park (1974) without taking into account the temperature dependence of the absorption cross section. Figure 5 and Figure 6 give examples of the reduction factors $R_b(O_2)$ and $R_b(M)$ and R(M) as a function of the O_2 total content. The computation is made with the parameters of the U.S Standard Atmosphere 1962 (COESA, 1962). The altitude scale corresponds to overhead sun conditions. The dashed curves give the results when the temperature is arbitrary assumed constant for a range of O_2 total content between 10^{17} cm^{-2} and 10^{23} cm^{-2}. Although the differences between the constant temperature curves and the exact computation is not very large in the case of $R_b(O_2)$ (see Figure 5), it is clear from Figure 6 that a constant temperature is an unrealistic assumption in the case of $R_b(M)$. Similar results are obtained for the other bands of the Schumann-Runge system.

When the reduction factors are known, the computation of the solar flux $\phi_b(z)$ reaching the height z, of the O_2 photodissociation coefficient $J_b(O_2)$ and of the photodissociation coefficient $J_b(M)$ for a minor constituent M is straightforward with the following expressions

$$\phi_b(z) = \phi_b(\infty)\, R_b(M)\, \exp\,[-\tau_b(O_3)] \tag{13}$$

$$J_b(O_2) = \phi_b(\infty)\, R_b(O_2)\, \exp\,[-\tau_b(O_3)] \tag{14}$$

$$J_b(M) = \phi_b(\infty)\, \sigma_b(M)\, R_b(M)\, \exp\,[-\tau_b(O_3)] \tag{15}$$

The effect resulting from the ozone absorption is taken into account by the factor $\exp\,[-\tau_b(O_3)]$ where $\tau_b(O_3)$ is the ozone optical depth at height z. The ozone absorption cross sections are taken from Ackerman (1971).

The addition of the 20 partial coefficients obtained from expression (14) leads to the O_2 photodissociation coefficient shown on Figure 7. The dashed curve represents the result obtained with the mean absorption cross sections shown on Figure 2. Errors larger than a

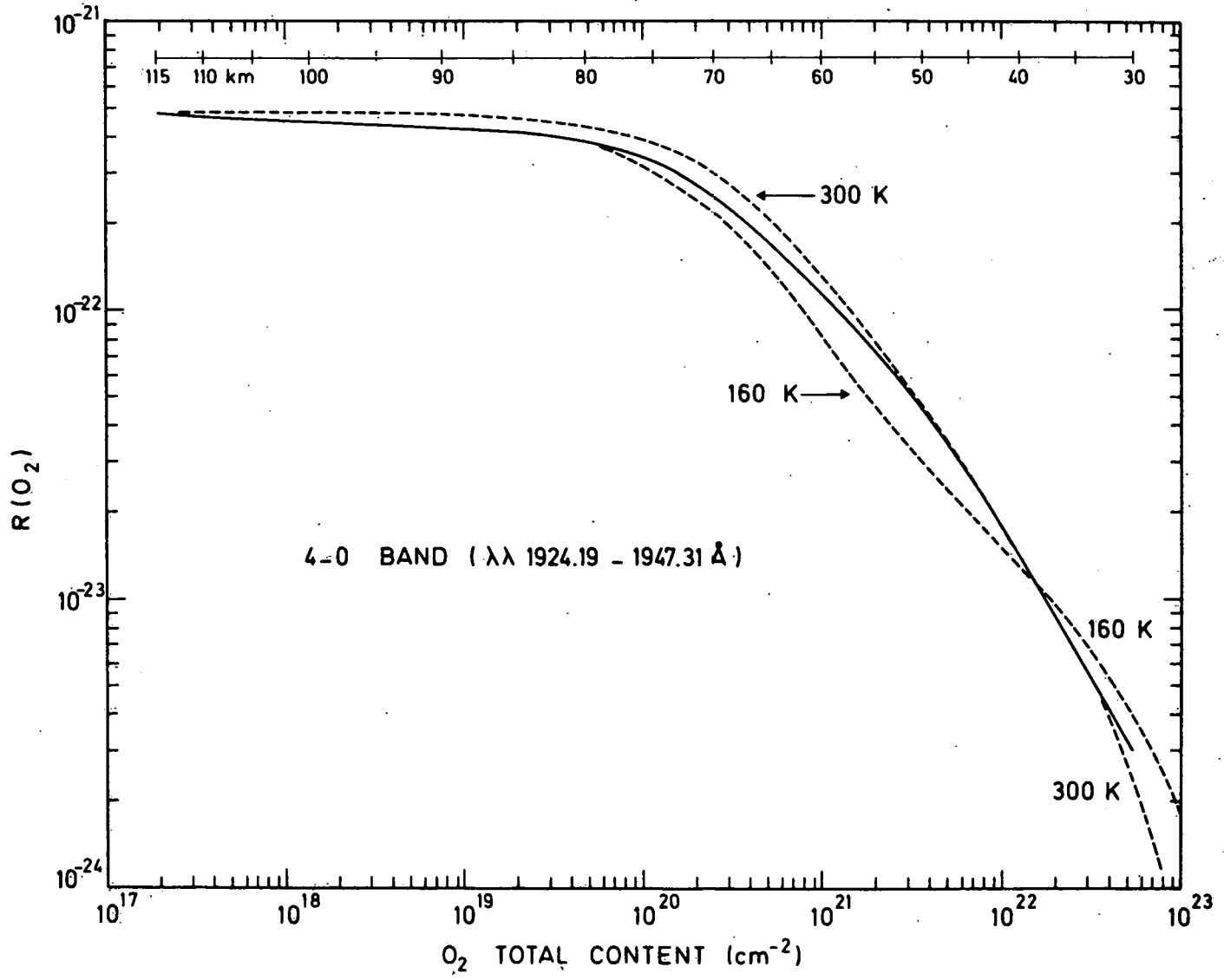

Fig. 5.- Comparison of the reduction factor $R_b(O_2)$ in the 4-0 band computed with temperature dependent cross sections (full curve) and with constant temperature (160 K and 300 K) cross sections. Overhead sun conditions.

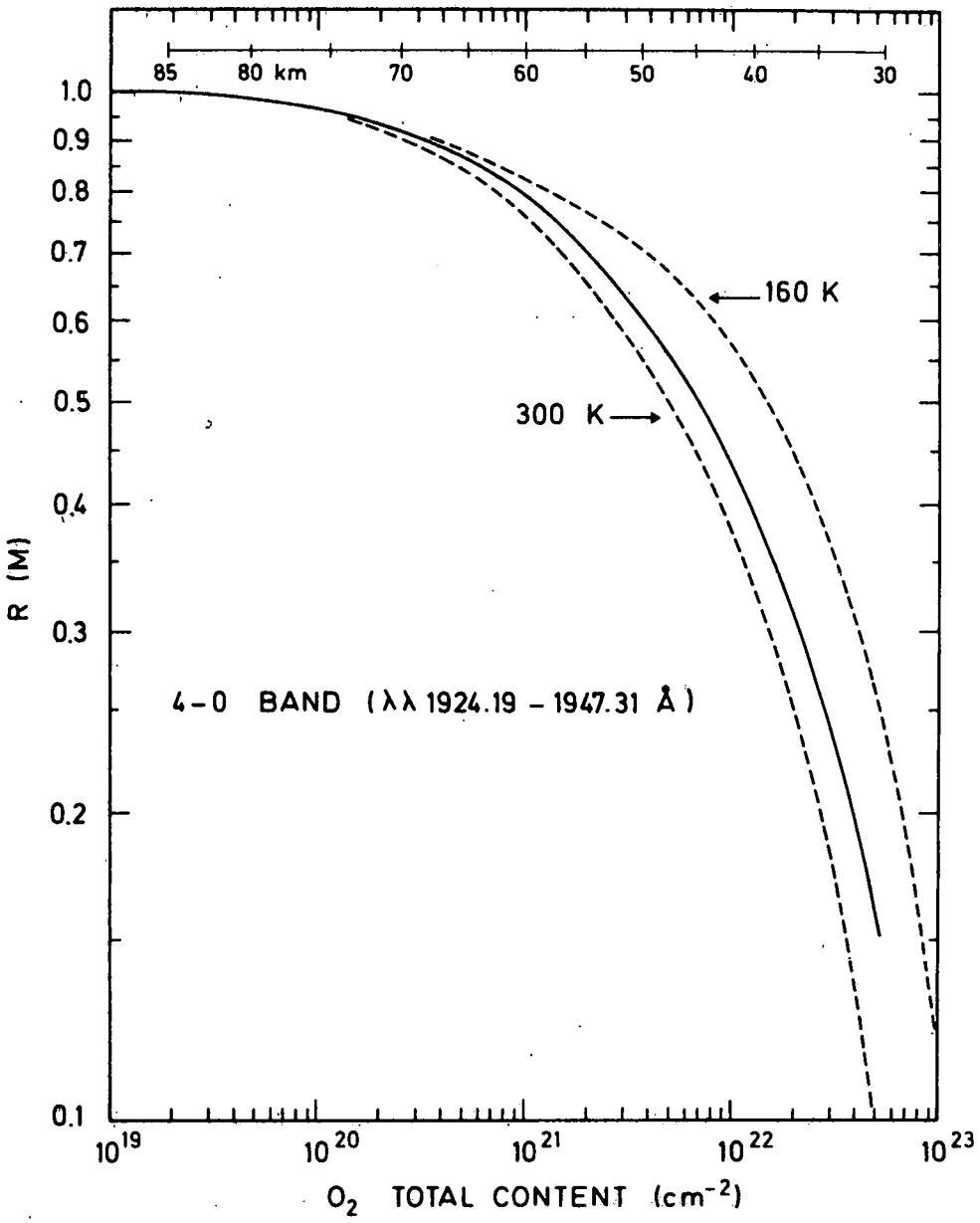

Fig. 6.- Comparison of the reduction factor $R_b(M)$ in the 4-0 band computed with temperature dependent cross sections (full curve) and with constant temperature (160 K and 300 K). Overhead sun conditions.

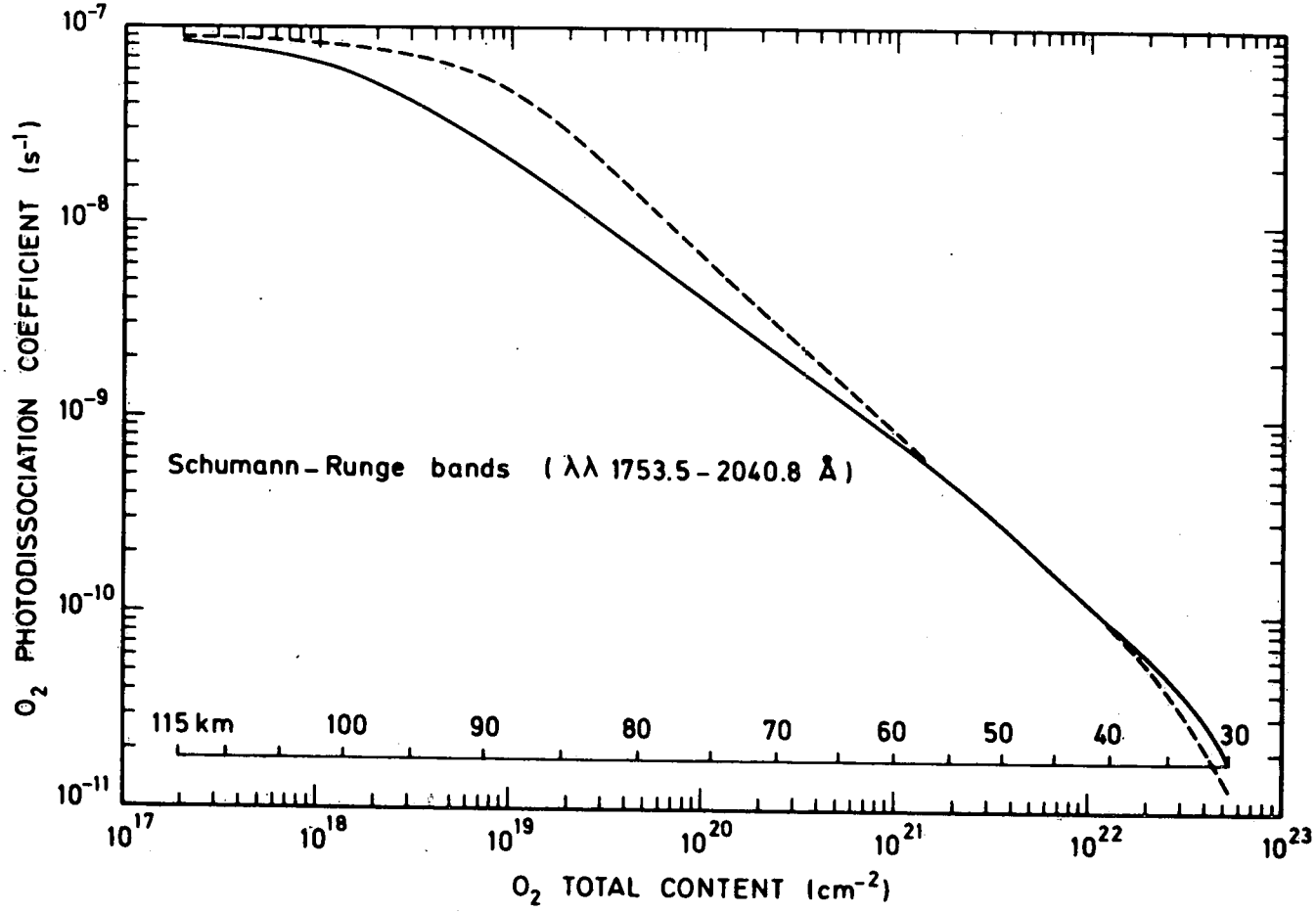

Fig. 7.- O_2 photodissociation coefficient in the Schumann-Runge bands as a function of the O_2 total content (full curve). The dashed curve is obtained with the mean absorption cross sections of Fig. 2. Overhead sun conditions.

factor of two appear over an extended range of the O_2 total content. In the upper stratosphere and lower mesosphere where the O_2 total content ranges from 10^{22} cm^{-2} to 10^{21} cm^{-2}, there is an excellent agreement. The ozone distribution adopted in the computation of Figure 7 is taken from Nicolet (1975) and it affects the results only below 40 km.

The photodissociation coefficients of several minor constituents, as shown in Figure 8, are obtained when expression (15) is used for each band of the Schumann-Runge system and when solar fluxes and absorption cross sections given in Table 1 are adopted. As in Figure 7, the dashed curves of Figure 8 are also computed with the mean cross sections defined in the preceeding section. It is clear that these mean cross sections cannot be used for any calculation of the photodissociation of minor constituents in the Schumann-Runge band spectral range. The use of mean cross sections always leads to a large underestimation of the photodissociation coefficients as it has already been noticed by Fang *et al.* (1974). The difference between the present values and those given by Kockarts (1971) for H_2O and by Banks and Kockarts (1973) for CO_2 is due essentially to the adoption of different values (Samain and Simon, 1976) for the solar fluxes.

In order to illustrate the role of the photodissociation in the spectral range of the Schumann-Runge bands, Figure 9 shows the vertical distribution of the ratio of the photodissociation coefficient in the Schumann-Runge wavelength region ($J_{S\text{-}R}$) and the total photodissociation coefficient (J_{total}). The solar fluxes outside of the Schumann-Runge bands have been adopted from Simon (1976). Between approximately 65 km and 95 km, the predissociation in the Schumann-Runge bands is the major dissociative process for O_2 for overhead sun conditions. In the stratosphere above 30 km, the photodissociation in the Schumann-Runge wavelength region contributes roughly by 50% to the photodissociation of nitric acid and of nitrous oxide. Below 60 km the photodissociation of CO_2 and H_2O is entirely due to solar radiation which penetrates in the Schumann-Runge bands. For H_2O_2, the contribution from the Schumann-Runge wavelength region is practically negligible.

Before introducing numerical approximations, it is useful to compare the absorption in the Herzberg continuum which starts at 2424 Å with the absorption in the Schumann–Runge bands which begin at 2040 Å. From $\lambda \simeq 2040$ Å, corresponding to the 0-0 band of

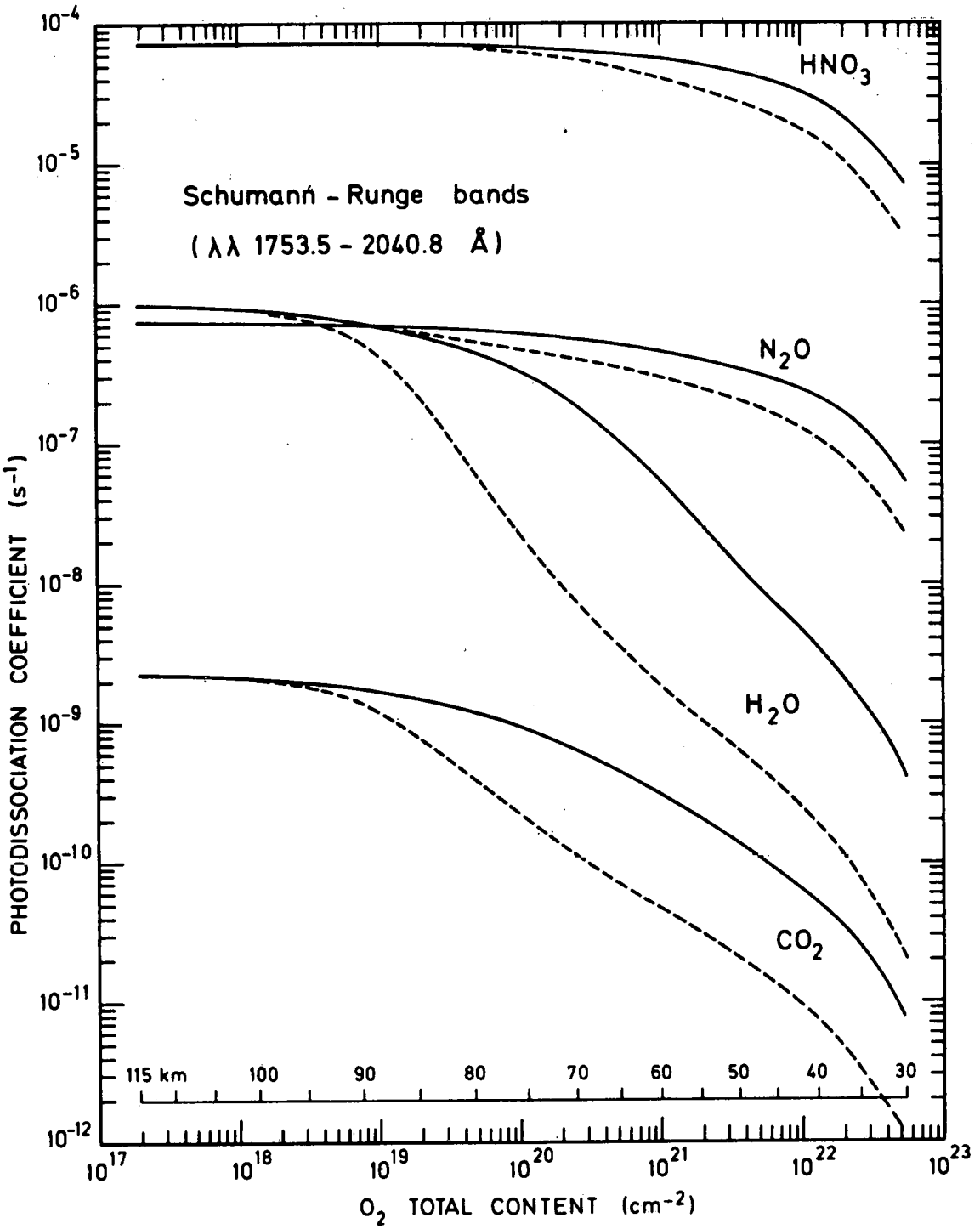

Fig. 8.- Photodissociation coefficients of HNO_3, N_2O, H_2O and CO_2 in the Schumann-Runge spectral region as a function of the O_2 total content (full curves). The dashed curves are obtained with the mean absorption cross sections of Fig. 2. Overhead sun conditions.

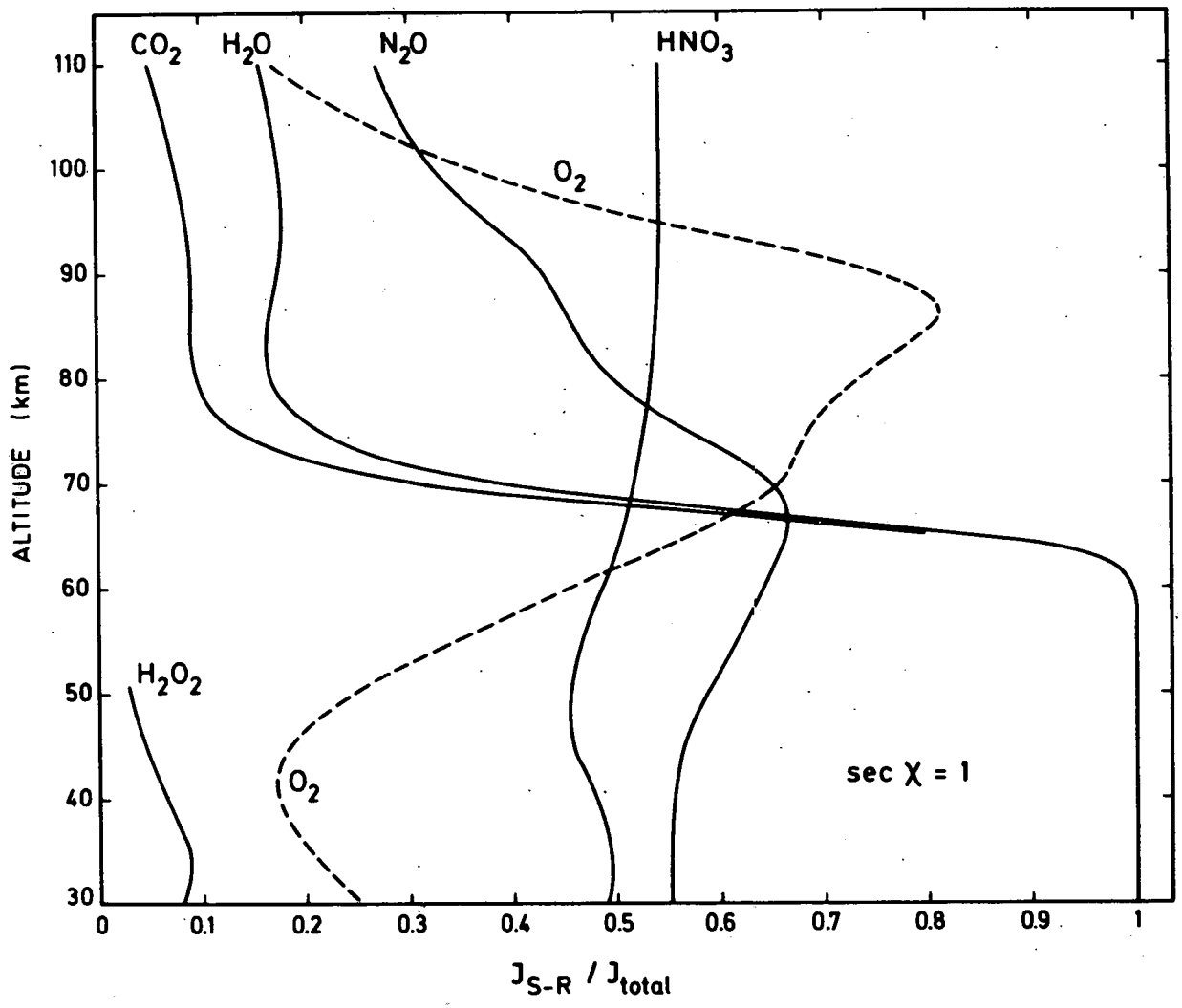

Fig. 9.- Ratios of photodissociation coefficients in the Schumann-Runge spectral range (J_{S-R}) and the total photodissociation coefficients (J_{total}) versus height for overhead sun conditions.

the Schumann-Runge system, the absorption cross-section of the Herzberg continuum increases from 1.15×10^{-23} cm^2 to its maximum of 1.30×10^{-23} cm^2 (Jarmain and Nicholls, 1967) near $\lambda = 1950$ Å which corresponds to the Schumann-Runge band 3-0. Since it is not yet established wether or not predissociation occurs in this spectral region, the contribution of the spectral range $\lambda\lambda$ 1950 - 2040 Å to the O_2 photodissociation must be studied with and without the action of a predissociation process in the Schumann-Runge bands 0-0 to 3-0 in addition to the normal photodissociation in the Herzberg continuum. Figure 10 shows the relative importance of the photodissociation due to the Schumann–Runge bands and to the Herzberg continuum between the threshold at 2424 Å and about 2040 Å where the 0-0 band starts. Two cases have been considered for the contribution of the Schumann-Runge bands : the full curve corresponds to complete predissociation in the whole band system and the dashed curve ignores predissociation in the 0-0 to 3-0 bands, but it takes into account the photodissociation in the underlying Herzberg continuum. In both cases absorption of the Herzberg continuum is included in the optical depth. Although the absence of predissociation in the 0-0 to 3-0 bands can reduce the photodissociation coefficient in the Schumann-Runge bands by 25% at 45 km, the reduction of the total O_2 photodissociation coefficient is, however, less than 5% over the whole height range, as can be seen on Figure 10.

As far as the minor constituents are concerned, the problem is different since it is only an absorption process which limits the penetration of solar radiation and affects in this way the value of the photodissociation coefficient. If the correct photodissociation coefficient of a minor constituent involving the total absorption in a certain band interval is designated by J_{S-R} (M) and if J_H (M) corresponds to the effect of the Herzberg continuum absorption in the same spectral range, the ratio $J_{S-R}(M)/J_H(M)$ does not depend on the absorption cross–section of the minor constituent. Such a ratio is given on Figure 11 as a function of height for the 0-0 to 3-0 bands. It appears that without the effect of the absorption by the lines of the Schumann-Runge bands 0-0 to 3-0, the photodissociation coefficient is always overestimated, i.e. $J_{S-R}(M)/J_H(M) < 1$. Below 2000 Å, absorption by the lines of the Schumann-Runge bands must be taken into account. It is, therefore, clear that the absorption of the Schumann-Runge bands plays an important role not only in the meso-sphere, but also in the stratosphere where several minor constituents are subject to photo-

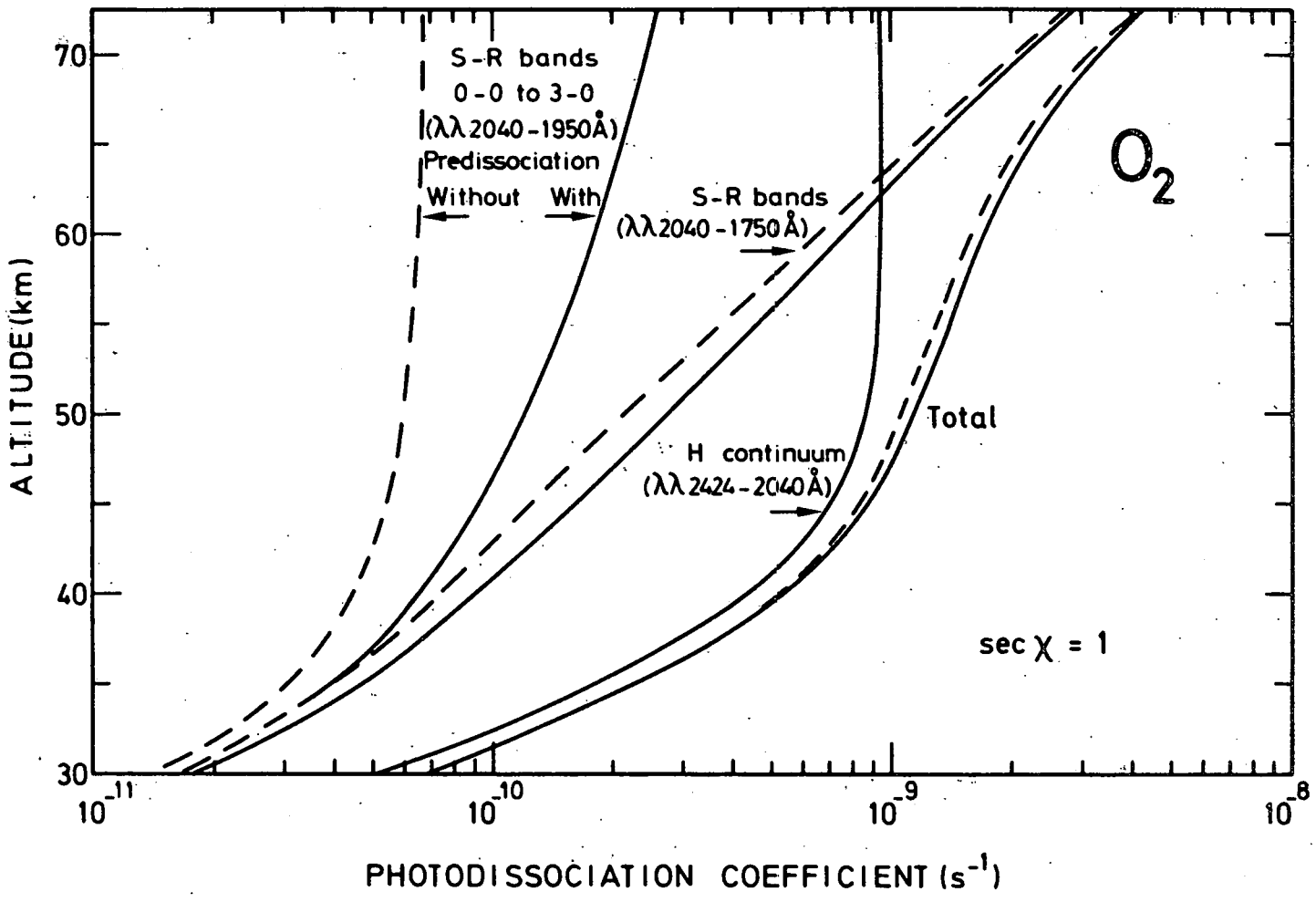

Fig. 10.- Vertical distribution of the O_2 photodissociation coefficient for overhead sun conditions. Contribution of the Herzberg continuum (H) from 2424 Å to 2040 Å and the Schumann-Runge bands (S-R) from 2040 Å to 1750 Å. The dashed curves correspond to the absence of predissociation in the 0-0 to 3-0 bands (λλ 2040 - 1950 Å) of the Schumann-Runge system.

dissociation processes at wavelengths shorter than 2000 A.

4. NUMERICAL APPROXIMATIONS FOR EACH BAND

It has been shown in the preceeding section how the exact reduction factors can be applied to the earth's atmosphere. Since $R_b(O_2)$ and $R_b(M)$ result from a detailed lengthy calculation, it is interesting to determine the approximation which can be valid for a large range of atmospheric conditions. A tabulation of the reduction factors as a function of height or O_2 total content is not very handy, since it requires important computer storage and subsequent interpolations. The temperature dependence of the transmittance of solar radiation and of the rate of dissociation is fitted by Hudson and Mahle (1972) through an empirical relation for which the numerical coefficients are given in tabular form as a function of the O_2 total content. Park (1974) gives a graphical representation of two sets of equivalent absorption cross sections as a function of the O_2 total content for one temperature. The technique adopted by Fang *et al.* (1974) is more practical but it requires, nevertheless, a numerical integration in order to obtain photodissociation coefficients as a function of the O_2 total content.

A good analytical approximation of the natural logarithm of the present reduction factors is given by

$$\ln R_b^*(x) = -a \exp [c_1(x - x_o) + c_2(x - x_o)^2 + \ldots + c_6(x - x_o)^6] \qquad (16)$$

where x is the natural logarithm of the total content of molecular oxygen. The numerical coefficients x_o, a, c_1 through c_6 are obtained through a least square fitting and are given in Tables II and III for the two reduction factors deduced for each band. These coefficients imply that the O_2 total content is expressed in molecules cm^{-2}. The coefficients $x_o = \int_{Z_o}^{\infty} n(O_2)\, ds$ have been chosen in a way such that the corresponding reduction factor is reduced by a factor of 1000. This implies that in each band, radiation is considered as completly absorbed when the average optical depth is greater than 6.9. For the bands $v' < 4$,

x_o corresponds to the height of 30 km for an overhead sun, since the computations have been stopped at that altitude. The highest altitude for which the present approximation is valid corresponds to an O_2 total content of 1.94×10^{17} cm^{-2}, i.e. an altitude of 115 km in the 45° N US Standard atmosphere for overhead sun conditions.

For a given O_2 total content, the reduction factors $R_b^*(O_2)$ and $R_b^*(M)$ can be immediately computed from expression (16) and Tables II and III. The error δ resulting from the use of expression (16) depends of the O_2 total content and has been computed every kilometer between the level x_o and 115 km from the expression

$$\delta = \frac{R_b^* - R_b}{R_b} \times 100\% \qquad (17)$$

This error can be positive or negative and its average value is practically zero as an obvious consequence of the least-square fitting procedure which leads to the coefficients of Tables II and III. An index of the accuracy of the analytical approximation (16) is then given by the standard deviation s (%) of the errors. The standard deviations s are given in Table IV for $R_b^*(M)$ and $R_b^*(O_2)$. It can be seen that the approximate expressions R_b^* represent rather well the correct results. The fit for $R_b^*(M)$ is usually better than for $R_b^*(O_2)$. When photodissociation coefficients are computed with $R_h^*(M)$ and $R_h^*(O_2)$ the agreement with the exact computations is such that it is impossible to distinguish both results on graphs like Figures 7 and 8. This implies that the approximate expressions can be used for modelling purposes, since the resulting error is much smaller than the errors involved in other parameters, such as the solar fluxes and the absorption cross sections of the minor constituents.

It is also possible to justify the validity of our approximation when the solar zenith distance changes and when other atmospheric models are used. Figure 12 shows the temperature distribution in the 45° N US Standard Atmosphere (COESA, 1962) and in the summer and winter models available in the US Standard Atmosphere Supplements (COESA, 1966).

TABLE II.- Coefficients for the reduction factors $R_b^*(M)$ in formula (16)

Band	x_o	a	c_1	c_2	c_3	c_4	c_5	c_6
19 - 0	48.5010	6.31710 (+0)*	6.08574 (-1)	2.97159 (-2)	5.09179 (-3)	—	—	—
18 - 0	47.8366	7.00050 (+0)	6.46284 (-1)	2.67214 (-2)	- 6.61165 (-3)	- 2.90019 (-3)	- 1.88591 (-4)	—
17 - 0	48.5010	6.89325 (+0)	5.76123 (-1)	6.46560 (-2)	1.20411 (-2)	4.25760 (-4)	—	—
16 - 0	48.3707	6.82169 (+0)	5.52366 (-1)	1.41801 (-2)	- 3.82459 (-3)	- 1.54704 (-3)	- 8.62462 (-5)	—
15 - 0	48.8862	6.84542 (+0)	7.04170 (-1)	7.90948 (-2)	4.21208 (-3)	- 1.05961 (-3)	- 7.41033 (-5)	—
14 - 0	49.1384	6.62131 (+0)	6.93027 (-1)	6.68624 (-2)	6.29880 (-3)	—	—	—
13 - 0	49.3872	6.74723 (+0)	6.28943 (-1)	- 2.45785 (-2)	- 2.08983 (-2)	- 3.09907 (-3)	- 1.24542 (-4)	—
12 - 0	49.5111	6.77155 (+0)	6.92233 (-1)	2.13024 (-2)	- 2.32312 (-3)	6.34869 (-4)	2.40848 (-4)	1.36871 (-5)
11 - 0	50.2588	6.74874 (+0)	5.26218 (-1)	- 2.16025 (-2)	- 8.38765 (-3)	- 1.20850 (-4)	1.50742 (-4)	9.13218 (-6)
10 - 0	50.9126	7.13157 (+0)	5.88084 (-1)	9.18305 (-3)	- 9.82008 (-4)	6.14794 (-4)	1.55366 (-4)	7.40423 (-6)
9 - 0	52.3372	6.38994 (+0)	3.17089 (-1)	- 4.48422 (-2)	- 5.76199 (-3)	- 3.15612 (-4)	—	—
8 - 0	52.3372	5.62872 (+0)	2.69400 (-1)	- 7.80898 (-2)	- 1.40938 (-2)	- 1.23486 (-3)	- 3.39746 (-5)	—
7 - 0	52.3372	3.95774 (+0)	4.37216 (-1)	1.35953 (-2)	3.25038 (-3)	6.66057 (-5)	—	—
6 - 0	52.3372	2.63932 (+0)	3.63251 (-1)	- 1.43244 (-2)	8.11499 (-4)	—	—	—
5 - 0	52.3372	2.39984 (+0)	4.44829 (-1)	- 1.42826 (-2)	- 1.53566 (-3)	- 2.53099 (-4)	1.67438 (-5)	1.90303 (-6)
4 - 0	52.3372	1.86306 (+0)	4.90040 (-1)	1.21828 (-2)	4.40861 (-3)	- 5.58066 (-4)	- 8.88669 (-5)	- 2.58811 (-6)
3 - 0	52.3372	1.33300 (+0)	5.61151 (-1)	3.78913 (-3)	8.28793 (-3)	5.50079 (-4)	—	—
2 - 0	52.3372	9.45868 (-1)	6.84962 (-1)	- 1.17630 (-2)	7.39342 (-3)	8.64629 (-4)	1.68263 (-5)	—
1 - 0	52.3372	7.09034 (-1)	7.35786 (-1)	- 7.74556 (-2)	- 6.54135 (-3)	—	—	—
0 - 0	52.3372	6.40222 (-1)	9.24003 (-1)	- 1.71422 (-2)	8.40830 (-4)	2.76026 (-4)	—	—

* $(+1) = 10^1$; $(-1) = 10^{-1}$

TABLE III.- Coefficients for the reduction factors $R_b^*(O_2)$ in formula (16)

Band	x_o	a	c_1	c_2	c_3	c_4	c_5	c_6
19 - 0	47.8366	5.11460 (+1)*	5.10382 (-2)	8.73943 (-3)	1.04447 (-3)	5.89092 (-5)	—	—
18 - 0	46.9705	5.00719 (+1)	4.43874 (-2)	5.00297 (-3)	3.79065 (-4)	2.46433 (-5)	—	—
17 - 0	47.1210	5.00818 (+1)	3.80646 (-2)	2.49528 (-3)	- 1.02661 (-5)	—	—	—
16 - 0	47.2689	5.04340 (+1)	4.63249 (-2)	7.09082 (-3)	8.98831 (-4)	5.77473 (-5)	—	—
15 - 0	47.6981	5.03652 (+1)	3.38745 (-2)	3.32142 (-3)	4.32553 (-4)	3.35514 (-5)	—	—
14 - 0	47.8366	5.02938 (+1)	3.51286 (-2)	5.31714 (-3)	8.15685 (-4)	5.34462 (-5)	—	—
13 - 0	48.1071	5.05610 (+1)	4.39864 (-2)	1.26616 (-2)	2.81490 (-3)	2.84044 (-4)	9.79660 (-6)	—
12 - 0	48.3707	5.10442 (+1)	5.99863 (-2)	2.82775 (-2)	9.18649 (-3)	1.52692 (-3)	1.24380 (-4)	4.01234 (-6)
11 - 0	48.7587	5.11875 (+1)	2.84639 (-2)	- 4.66058 (-3)	- 4.55939 (-3)	- 1.20694 (-3)	- 1.34151 (-4)	- 5.33233 (-6)
10 - 0	49.2632	5.16385 (+1)	3.80068 (-2)	8.98509 (-3)	1.73130 (-3)	1.18619 (-4)	- 3.39860 (-6)	- 4.54339 (-7)
9 - 0	49.7590	5.22077 (+1)	4.71498 (-2)	1.56032 (-2)	3.45399 (-3)	3.45446 (-4)	1.23091 (-5)	—
8 - 0	50.1323	5.24801 (+1)	4.04241 (-2)	1.14692 (-2)	2.68444 (-3)	3.24591 (-4)	1.81548 (-5)	3.77777 (-7)
7 - 0	50.9126	5.32532 (+1)	2.92527 (-2)	2.18557 (-3)	- 1.82273 (-4)	- 8.43583 (-5)	- 9.19628 (-6)	- 3.19482 (-7)
6 - 0	51.7482	5.39973 (+1)	2.55970 (-2)	1.37135 (-3)	1.35395 (-5)	—	—	—
5 - 0	52.3372	5.45428 (+1)	2.89681 (-2)	3.89198 (-3)	6.32160 (-4)	6.86338 (-5)	3.25533 (-6)	4.72141 (-8)
4 - 0	52.3372	5.40782 (+1)	1.81043 (-2)	- 9.49775 (-4)	- 3.91127 (-4)	- 2.52678 (-5)	- 4.25174 (-7)	—
3 - 0	52.3372	5.37578 (+1)	1.76096 (-2)	8.60701 (-4)	- 8.73800 (-5)	- 6.32969 (-6)	—	—
2 - 0	52.3372	5.35484 (+1)	1.56696 (-2)	2.24308 (-3)	1.32230 (-4)	2.57769 (-6)	—	—
1 - 0	52.3372	5.32918 (+1)	8.44393 (-3)	1.44896 (-3)	9.75944 (-5)	2.12883 (-6)	—	—
0 - 0	52.3372	5.33607 (+1)	9.95270 (-3)	3.37492 (-3)	5.50237 (-4)	4.24324 (-5)	1.23625 (-6)	—

* $(+1) = 10^1$; $(-1) = 10^{-1}$.

TABLE IV.- Standard deviation for the band interval approximations $R_b^*(M)$ and $R_b^*(O_2)$

Band	$s[R_b^*(M)]$ (%)	$s[R_b^*(O_2)]$ (%)	Band	$s[R_b^*(M)]$ (%)	$s[R_b^*(O_2)]$ (%)
19 - 0	1.03	2.77	9 - 0	4.99	4.07
18 - 0	2.04	4.55	8 - 0	6.57	3.98
17 - 0	1.27	2.72	7 - 0	2.53	4.82
16 - 0	1.63	1.96	6 - 0	1.14	7.22
15 - 0	0.68	2.74	5 - 0	0.84	4.68
14 - 0	1.67	3.45	4 - 0	0.45	2.92
13 - 0	1.13	2.19	3 - 0	0.86	2.98
12 - 0	0.35	4.47	2 - 0	0.81	1.69
11 - 0	0.88	3.90	1 - 0	0.92	3.60
10 - 0	4.04	2.32	0 - 0	0.40	1.52

For a specific model, variations of the solar zenith distance imply variations of the O_2 total content. Since the last quantity is temperature dependent, different absorption cross sections should be used in the optical depth given by equation (5). Figure 12 indicates that, for total contents greater than 10^{18} cm^{-2}, a variation of a factor of 4 in the total content of the 45°N model implies always a temperature variation smaller than 30 K, i.e. a neglible variation in the absorption cross section. Variations of the solar zenith distance between 0° and 75° are therefore, well represented by total content variations in expression (16). Isolated sunrise and sunset phenomena are better described by detailed computations.

Adoption of other atmospheric models, for example the 45°N July or January models could a *priori* lead to variations in the reduction factors since the temperature distribution is different over the whole height range. The exact reduction factor $R_b(O_2)$ computed for the 6-0 band with equation (12) is given in Figure 13 for the three models shown in Figure 12 and it is clear that the differences are practically negligible. A similar comparison is presented in Figure 14 for the reduction factor $R_b(M)$ computed for the 9-0 band with equation (11). It is only for optical depths greater than 4.6 that sensible differences occur. The bands 6-0 and 9-0 have been chosen for Figures 13 and 14 since they correspond to relatively large errors ($\geq 5\%$) in the numerical approximation (see Table IV). It appears, nevertheless, that the numerical coefficients given in Tables II and III, can be used for a wide range of atmospheric models.

5. NUMERICAL APPROXIMATIONS FOR $\Delta\nu = 500\ cm^{-1}$ and $\Delta\lambda = 10$ Å

The subdivision of the Schumann-Runge spectral range adopted in the preceding sections is based on the physical structure (individual bands) of the absorption cross section of molecular oxygen and the penetration of solar radiation and photodissociation coefficients have been determined using the solar flux available at the top of the atmosphere. Since solar flux measurements are often averaged over specific wavelength or wavenumber intervals, the analysis, which was developped in section 4, is, therefore, extended for usual applications with 500 cm^{-1} or 10 Å intervals. Expressions (4) to (17) can be used

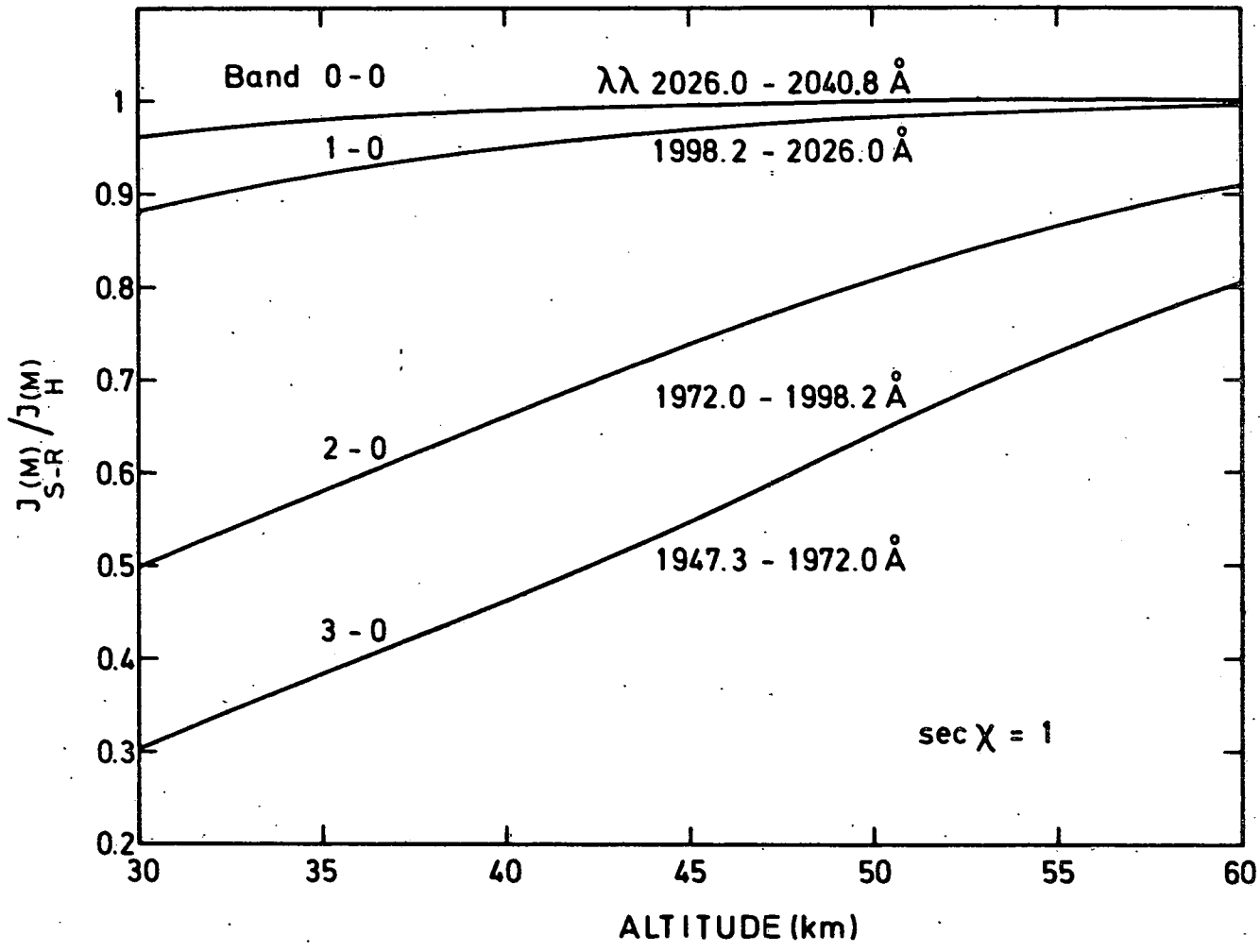

Fig. 11.- Ratio of the correct photodissociation coefficient $J_{S-R}(M)$ and the coefficient $J_H(M)$ resulting from absorption by the Herzberg continuum in the 0-0, 1-0, 2-0 and 3-0 bands of the Schumann-Runge system. The curves are valid for any minor constituent with constant absorption cross section over each band interval. Overhead sun conditions.

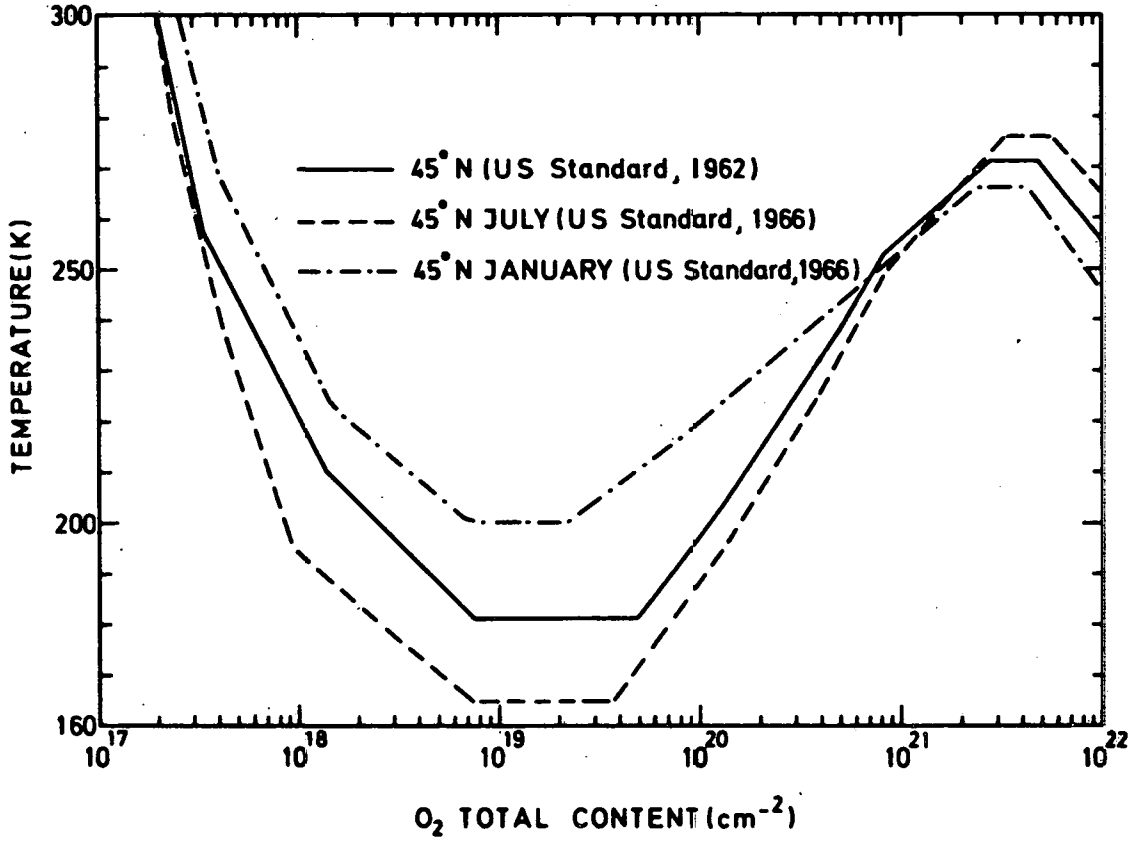

Fig. 12.- Temperature distribution in three 45°N atmospheric models as a function of the vertical O_2 total content.

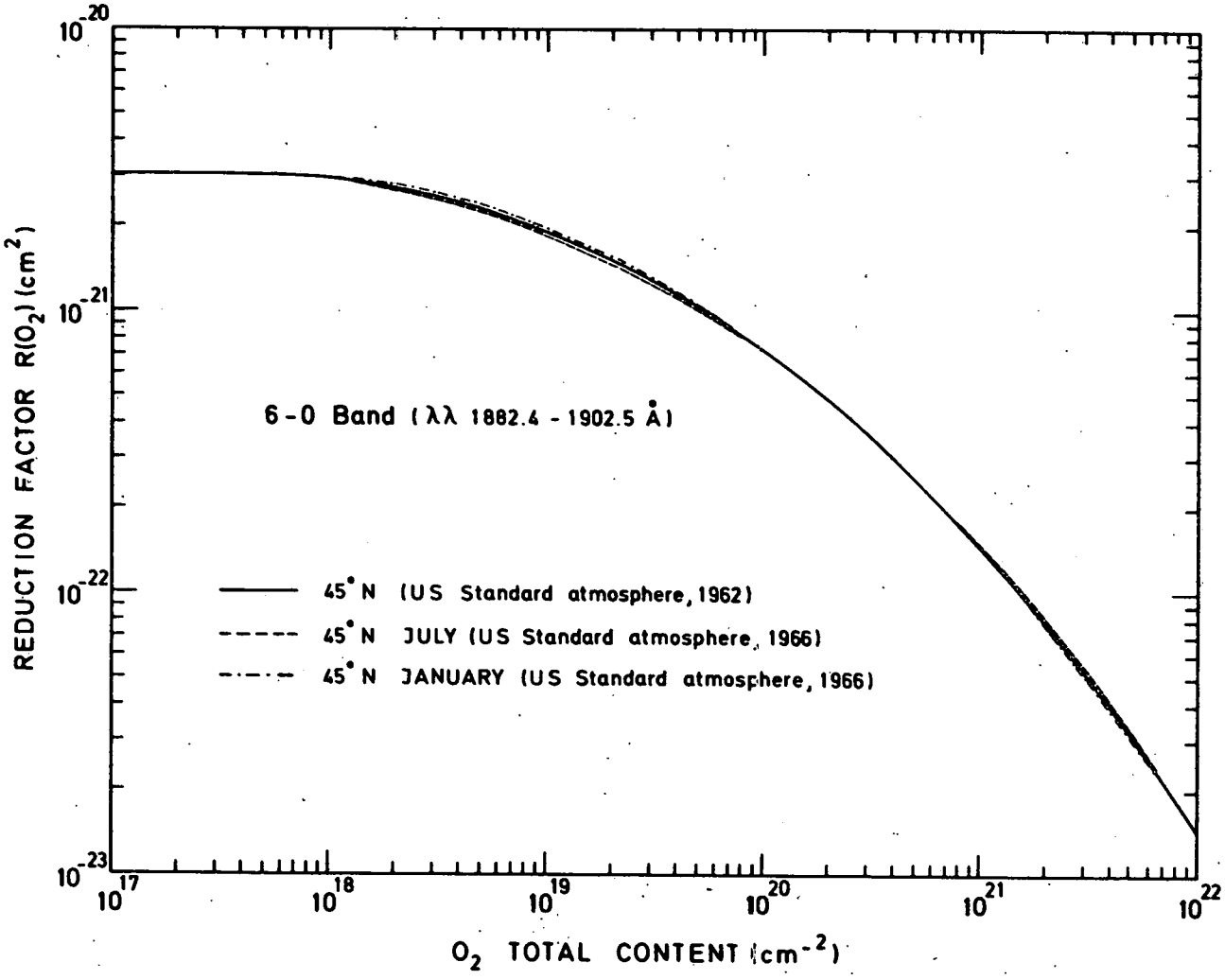

Fig. 13.- Comparison of the reduction factor $R_b(O_2)$ in the 6-0 band for three 45°N atmospheric models as a function of the O_2 total content.

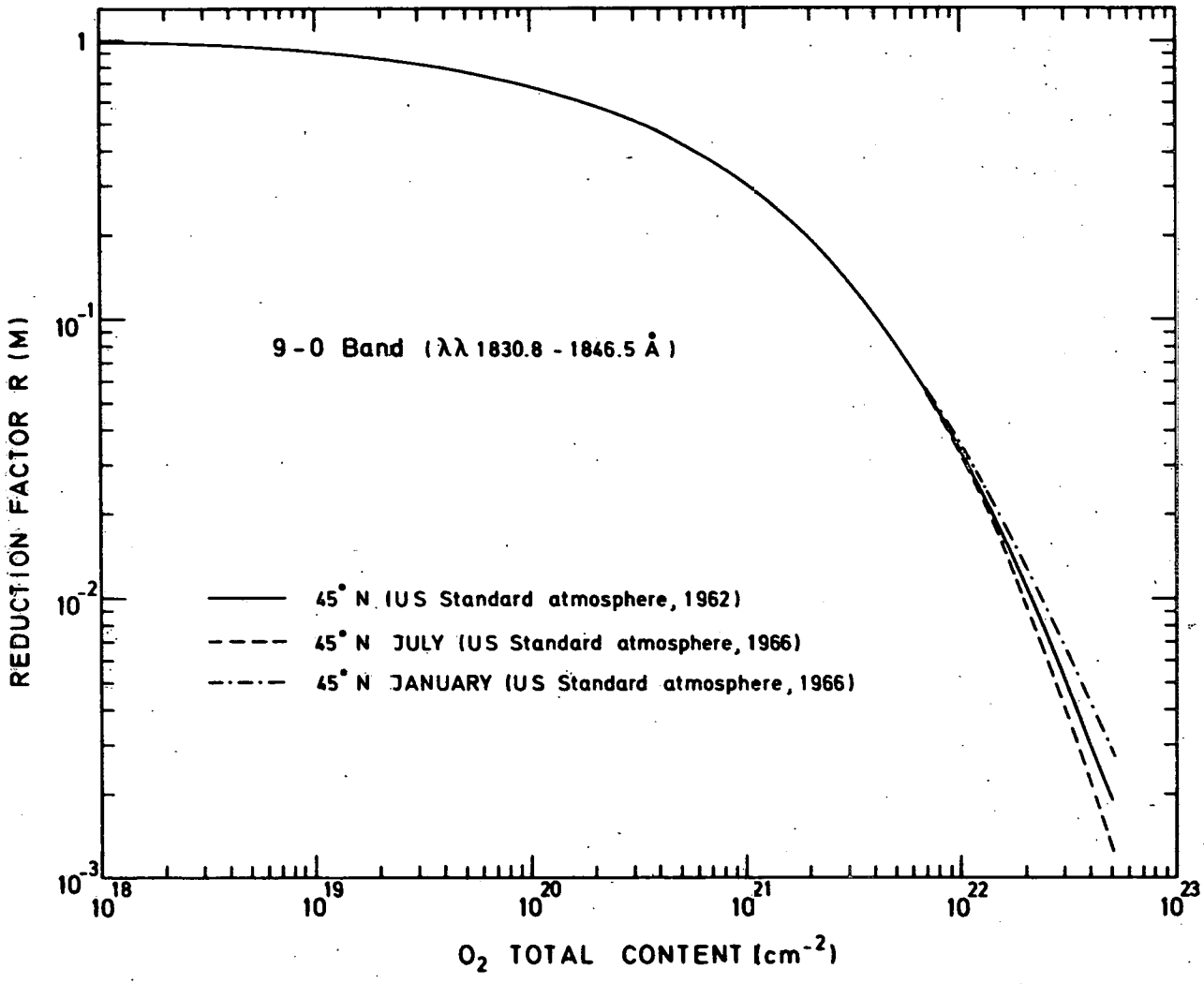

Fig. 14.- Comparison of the reduction factor $R_b(M)$ in the 9-0 band for three 45^0N atmospheric models as a function of the O_2 total content.

for such an extension when the index b now refers to the wavenumber interval $\Delta\nu = 500\ cm^{-1}$ or to the wavelength interval $\Delta\lambda = 10$ Å and when n_b is the number of subintervals characterized by a width of $0.5\ cm^{-1}$ in the intervals $\Delta\nu$ or $\Delta\lambda$.

The reduction factors $R_{\Delta\nu}(M)$, $R_{\Delta\nu}(O_2)$, $R_{\Delta\lambda}(M)$ and $R_{\Delta\lambda}(O_2)$ are first computed with expressions (11) and (12). Then the coefficients of the analytical approximation (16) are similarly determined as for the band intervals. The approximate reduction factors $R^*_{\Delta\nu}(M)$ and $R^*_{\Delta\nu}(O_2)$ can now be computed with the coefficients given in Tables V and VI, respectively. The computations have been made with the 45°N US Standard Atmosphere (COESA, 1962). The standard deviations for each $500\ cm^{-1}$ interval are given in Table VII. For wavelength intervals of 10 Å, the coefficients of $R^*_{\Delta\lambda}(M)$ and $R^*_{\Delta\lambda}(O_2)$ are presented in Tables VIII and IX, respectively, with the standard deviations in Table X. It appears from Tables IV, VII, and X that the standard deviation never exceeds 10%. Most values are even smaller then 5%. The accuracy is, however, not identical for any type of subdivision of the Schumann-Runge spectral range. The variability of the standard deviations in the intervals of the same type (band, $500\ cm^{-1}$, 10 Å) is an indication of the complexity of the structure in the Schumann-Runge bands. In particular when an interval overlaps with two bands, the standard deviation of the approximation is usually higher. For the case of the band intervals, the error increases when one or two band origin of the v" = 1 progression falls in this interval. Finally, it appears that the standard deviation is usually higher for the $R^*(O_2)$ reduction factors as a consequence of the appearance of the O_2 absorption cross section in front of the exponential in equation (12).

The choice of R^*_b, $R^*_{\Delta\nu}$ or $R^*_{\Delta\lambda}$ must be guided by the physical problem which is studied and by the precision involved in other parameters such as solar fluxes or absorption cross sections.

TABLE V.- Coefficients for the reduction factors $R^*_{\Delta\nu}(M)$ ($\Delta\nu = 500\ cm^{-1}$)

Interval (cm^{-1})	x_o	a	c_1	c_2	c_3	c_4	c_5	c_6
56500 - 57000	48.3707	6.84796 (+0)*	5.17316 (-1)	8.59061 (-3)	- 3.72072 (-3)	- 1.50404 (-3)	- 8.50021 (-5)	—
56000 - 56500	49.0127	6.53186 (+0)	6.49898 (-1)	5.81672 (-2)	5.98594 (-3)	—	—	—
55500 - 56000	49.5111	6.84941 (+0)	6.66003 (-1)	- 8.07720 (-3)	- 1.01234 (-2)	- 2.88266 (-4)	1.83032 (-4)	1.20649 (-5)
55000 - 55500	50.1323	6.54328 (+0)	4.94888 (-1)	- 3.45895 (-2)	- 1.12340 (-2)	- 2.22054 (-4)	1.86201 (-4)	1.17659 (-5)
54500 - 55000	50.7790	6.61757 (+0)	4.96086 (-1)	- 4.02125 (-2)	- 1.58932 (-2)	- 2.04106 (-3)	- 7.45240 (-5)	—
54000 - 54500	52.3372	6.46996 (+0)	3.01154 (-1)	- 5.65770 (-2)	- 9.71457 (-3)	- 8.70772 (-4)	- 2.36123 (-5)	—
53500 - 54000	52.3372	5.66059 (+0)	2.88223 (-1)	- 6.36151 (-2)	- 9.79217 (-3)	- 8.87904 (-4)	- 2.61077 (-5)	—
53000 - 53500	52.3372	3.82674 (+0)	4.08489 (-1)	- 6.77337 (-4)	3.02650 (-3)	1.09148 (-4)	—	—
52500 - 53000	52.3372	2.50743 (+0)	3.36617 (-1)	- 4.89806 (-2)	- 3.99197 (-3)	3.19888 (-5)	5.69852 (-5)	3.14619 (-6)
52000 - 52500	52.3372	2.21706 (+0)	4.46436 (-1)	- 2.92693 (-2)	- 1.07835 (-3)	- 4.06946 (-4)	- 4.34128 (-5)	- 1.15593 (-6)
51500 - 52000	52.3372	2.25964 (+0)	4.39618 (-1)	- 5.79418 (-4)	3.61300 (-3)	- 4.70989 (-4)	- 7.80044 (-5)	- 2.38741 (-6)
51000 - 51500	52.3372	1.62727 (+0)	5.25292 (-1)	- 1.36387 (-2)	2.51229 (-3)	- 3.41931 (-4)	- 6.22044 (-5)	- 1.75418 (-6)
50500 - 51000	52.3372	1.15386 (+0)	6.73839 (-1)	- 1.61677 (-2)	4.81976 (-3)	4.44662 (-4)	—	—
50000 - 50500	52.3372	8.37997 (-1)	7.83500 (-1)	- 4.04270 (-2)	2.06058 (-3)	6.63043 (-4)	1.70475 (-5)	—
49500 - 50000	52.3372	7.34295 (-1)	8.69102 (-1)	- 1.21049 (-2)	6.09572 (-3)	9.62943 (-4)	2.57319 (-5)	—
49000 - 49500	52.3372	6.34568 (-1)	9.54356 (-1)	7.95421 (-3)	7.64268 (-3)	9.97614 (-4)	2.47973 (-5)	—

* $(+1) = 10^1$; $(-1) = 10^{-1}$

TABLE VI.- Coefficients for the reduction factors $R^{*}_{\Delta\nu}(O_2)$ ($\Delta\nu = 500\ cm^{-1}$)

Interval (cm^{-1})	x_o	a	c_1	c_2	c_3	c_4	c_5	c_6
56500 - 57000	47.1210	5.02877 (+1)*	4.82355 (-2)	8.27089 (-3)	1.15739 (-3)	7.73906 (-5)	—	—
56000 - 56500	47.8366	5.05677 (+1)	4.16742 (-2)	8.62389 (-3)	1.70708 (-3)	1.66265 (-4)	5.22380 (-6)	—
55500 - 56000	48.3707	5.10464 (+1)	5.91157 (-2)	2.40099 (-2)	6.11691 (-3)	7.01218 (-4)	2.88977 (-5)	—
55000 - 55500	48.6303	5.11271 (+1)	3.29493 (-2)	- 8.68988 (-4)	- 3.42549 (-3)	- 1.09137 (-3)	- 1.34276 (-4)	- 5.72530 (-6)
54500 - 55000	49.2632	5.18149 (+1)	4.03702 (-2)	8.39479 (-3)	1.20197 (-3)	7.45130 (-6)	- 1.34654 (-5)	- 8.01332 (-7)
54000 - 54500	49.8830	5.25076 (+1)	5.05408 (-2)	1.68231 (-2)	3.76192 (-3)	3.86970 (-4)	1.42579 (-5)	—
53500 - 54000	50.3867	5.29051 (+1)	3.70815 (-2)	5.85835 (-3)	7.38473 (-4)	5.21511 (-5)	1.32429 (-6)	—
53000 - 53500	51.3230	5.39594 (+1)	3.69966 (-2)	5.84476 (-3)	7.89350 (-4)	6.37308 (-5)	1.98711 (-6)	—
52500 - 53000	52.1884	5.47078 (+1)	3.47011 (-2)	5.51635 (-3)	8.45727 (-4)	8.53671 (-5)	4.11990 (-6)	6.85472 (-8)
52000 - 52500	52.3372	5.43298 (+1)	2.55053 (-2)	1.66027 (-3)	- 3.21809 (-5)	- 4.82309 (-6)	—	—
51500 - 52000	52.3372	5.43850 (+1)	2.15633 (-2)	- 9.10283 (-4)	- 4.89103 (-4)	- 3.73518 (-5)	- 8.54613 (-7)	—
51000 - 51500	52.3372	5.38929 (+1)	1.91196 (-2)	1.69782 (-4)	- 3.25458 (-4)	- 3.07342 (-5)	- 8.22557 (-7)	—
50500 - 51000	52.3372	5.35620 (+1)	1.69056 (-2)	2.10918 (-3)	8.48166 (-5)	—	—	—
50000 - 50500	52.3372	5.33348 (+1)	1.15487 (-2)	2.14539 (-3)	1.43383 (-4)	2.65172 (-6)	—	—
49500 - 50000	52.3372	5.34000 (+1)	1.13954 (-2)	2.23775 (-3)	2.39814 (-5)	- 3.71615 (-5)	- 3.92715 (-6)	- 1.23474 (-7)
49000 - 49500	52.3372	5.32813 (+1)	5.89039 (-3)	1.16632 (-3)	9.38987 (-5)	2.63348 (-6)	—	—

* $(+1) = 10^{1}$; $(-1) = 10^{-1}$.

TABLE VII.- Standard deviation for the 500 cm^{-1} approximations $R^*_{\Delta\nu}(M)$ and $R^*_{\Delta\nu}(O_2)$

Interval (cm^{-1})	$s[R^*_{\Delta\nu}(M)]$ (%)	$s[R^*_{\Delta\nu}(O_2)]$ (%)	Interval (cm^{-1})	$s[R^*_{\Delta\nu}(M)]$ (%)	$s[R^*_{\Delta\nu}(O_2)]$ (%)
56500 - 57000	1.37	2.87	52500 - 53000	1.30	6.49
56000 - 56500	0.44	1.55	52000 - 52500	0.94	4.89
55500 - 56000	0.78	4.64	51500 - 52000	0.54	2.60
55000 - 55500	0.99	3.55	51000 - 51500	0.73	2.07
54500 - 55000	1.27	2.36	50500 - 51000	0.39	3.72
54000 - 54500	5.78	4.09	50000 - 50500	0.44	4.67
53500 - 54000	6.76	7.80	49500 - 50000	0.43	0.67
53000 - 53500	2.08	5.18	49000 - 49500	0.40	2.67

TABLE VIII.- Coefficients for the reduction factors $R^{*}_{\Delta\lambda}(M)$ ($\Delta\lambda = 10$ Å)

Interval (Å)	x_o	a	c_1	c_2	c_3	c_4	c_5	c_6
1750 - 1760	48.2394	6.89763 (+0)*	5.29106 (-1)	5.67145 (-2)	1.60166 (-2)	4.44083 (-3)	8.40779 (-4)	5.01998 (-5)
1760 - 1770	48.3707	6.67932 (+0)	5.63736 (-1)	6.28478 (-2)	1.89533 (-2)	3.28456 (-3)	4.01096 (-4)	1.88421 (-5)
1770 - 1780	48.7587	6.49036 (+0)	6.72570 (-1)	5.97308 (-2)	6.216:5 (-3)	—	—	—
1780 - 1790	49.1384	6.46131 (+0)	6.58662 (-1)	3.47022 (-3)	- 1.09451 (-2)	- 1.38507 (-3)	3.16800 (-5)	5.81154 (-6)
1790 - 1800	49.5111	6.74455 (+0)	6.60024 (-1)	1.87822 (-2)	- 3.03357 (-3)	4.64532 (-4)	2.25992 (-4)	1.32604 (-5)
1800 - 1810	49.3872	6.67780 (+0)	6.72745 (-1)	3.81980 (-3)	- 1.77364 (-2)	- 3.49056 (-3)	- 1.67210 (-4)	—
1810 - 1820	50.2588	6.56436 (+0)	5.69372 (-1)	- 2.28925 (-2)	- 1.11467 (-2)	- 4.74513 (-4)	1.48286 (-4)	1.00247 (-5)
1820 - 1830	50.9126	6.66317 (+0)	5.84378 (-1)	- 1.51955 (-2)	- 2.28127 (-3)	2.02568 (-4)	6.49102 (-5)	2.96791 (-6)
1830 - 1840	50.6468	7.09088 (+0)	6.60362 (-1)	5.00243 (-2)	4.95675 (-3)	3.27498 (-5)	—	—
1840 - 1850	52.3372	6.13304 (+0)	4.07111 (-1)	- 3.88234 (-2)	- 1.21131 (-2)	- 1.36375 (-3)	- 4.28120 (-5)	—
1850 - 1860	52.0404	6.73366 (+0)	3.01091 (-1)	- 9.64724 (-2)	- 8.64758 (-3)	5.31552 (-4)	1.30406 (-4)	5.30821 (-6)
1860 - 1870	52.3372	5.02651 (+0)	2.68855 (-1)	- 4.51007 (-2)	- 8.30801 (-3)	- 9.71517 (-4)	- 3.28893 (-5)	—
1870 - 1880	52.3372	3.35811 (+0)	3.58322 (-1)	- 2.87486 (-2)	6.41145 (-3)	5.28891 (-4)	- 3.36908 (-5)	- 2.75414 (-6)
1880 - 1890	52.3372	4.95636 (+0)	3.80234 (-1)	- 1.66185 (-2)	- 3.41757 (-3)	- 6.57498 (-4)	- 2.72453 (-5)	—
1890 - 1900	52.3372	1.97465 (+0)	4.75264 (-1)	- 1.09092 (-2)	8.90634 (-3)	1.46761 (-4)	- 1.20909 (-4)	- 6.49139 (-6)
1900 - 1910	52.3372	5.39459 (+0)	4.64390 (-1)	- 1.53222 (-2)	- 2.31276 (-3)	- 2.73232 (-4)	2.25483 (-5)	2.11368 (-6)
1910 - 1920	52.3372	1.81992 (+0)	5.08220 (-1)	- 1.13600 (-2)	1.14126 (-2)	3.40578 (-4)	- 1.34649 (-4)	- 7.55946 (-6)
1920 - 1930	52.3372	3.06585 (+0)	4.02512 (-1)	7.83849 (-3)	6.28983 (-3)	- 1.73235 (-4)	- 6.29372 (-5)	- 2.21684 (-6)
1930 - 1940	52.3372	1.85962 (+0)	3.64911 (-1)	- 1.14010 (-1)	- 6.34984(-3)	—	—	—
1940 - 1950	52.3372	1.51564 (+0)	5.28202 (-1)	9.55208 (-3)	7.91041 (-3)	4.34474 (-4)	—	—
1950 - 1960	52.3372	1.60222 (+0)	5.11932 (-1)	- 2.61144 (-2)	4.95775 (-3)	1.65694 (-4)	- 5.11283 (-5)	- 2.51486 (-6)
1960 - 1970	52.3372	9.71685 (-1)	5.12511 (-1)	- 1.62117 (-1)	- 1.46720 (-2)	- 2.77276 (-4)	—	—
1970 - 1980	52.3372	1.37699 (+0)	6.26462 (-1)	- 7.08644 (-3)	5.68126 (-3)	3.99301 (-4)	—	—
1980 - 1990	52.3372	8.84565 (-1)	7.26460 (-1)	- 7.76640 (-2)	- 4.84521 (-3)	7.28988 (-5)	—	—
1990 - 2000	52.3372	8.66214 (-1)	1.00177 (+0)	4.51336 (-2)	1.03045 (-2)	6.41182 (-4)	—	—
2000 - 2010	52.3372	8.84123 (-1)	9.31330 (-1)	1.04577 (-2)	5.95152 (-3)	4.78163 (-4)	—	—
2010 - 2020	52.3372	6.77989 (-1)	1.00667 (+0)	1.97533 (-2)	6.32736 (-3)	5.00822 (-4)	—	—
2020 - 2030	52.3372	6.94593 (-1)	1.08332 (+0)	5.28970 (-2)	1.05677 (-2)	6.66814 (-4)	—	—
2030 - 2040	52.3372	6.51117 (-1)	1.03060 (+0)	3.03642 (-2)	7.70258 (-3)	5.57472 (-4)	—	—
2040 - 2050	52.3372	6.16626 (-1)	1.05655 (+0)	4.11376 (-2)	9.08845 (-3)	6.15747 (-4)	—	—

* $(+1) = 10^{1}$; $(-1) = 10^{-1}$.

TABLE IX.- Coefficients for the reduction factors $R^{*}_{\Delta\lambda}(O_2)$ ($\Delta\lambda = 10$ Å)

Interval (Å)	x_o	a	c_1	c_2	c_3	c_4	c_5	c_6
1750 - 1760	46.8173	4.98284 (+1)*	3.87574 (-2)	9.17924 (-3)	4.07267 (-3)	7.80514 (-4)	4.73601 (-5)	—
1760 - 1770	47.1210	5.02232 (+1)	5.00733 (-2)	1.53258 (-2)	5.59964 (-3)	1.18880 (-3)	1.22784 (-4)	4.97235 (-6)
1770 - 1780	47.6981	5.03908 (+1)	3.98650 (-2)	6.50488 (-3)	9.45939 (-4)	5.98214 (-5)	—	—
1780 - 1790	48.1071	5.06646 (+1)	4.08847 (-2)	8.19503 (-3)	1.26973 (-3)	7.54648 (-5)	—	—
1790 - 1800	48.3707	5.09270 (+1)	3.94964 (-2)	7.51466 (-3)	1.15582 (-3)	6.89678 (-5)	—	—
1800 - 1810	48.3707	5.09869 (+1)	3.91533 (-2)	6.60149 (-3)	9.50775 (-4)	5.79830 (-5)	—	—
1810 - 1820	49.0127	5.15103 (+1)	3.79382 (-2)	7.42674 (-3)	1.33775 (-3)	1.17154 (-4)	3.26677 (-6)	—
1820 - 1830	49.6350	5.20520 (+1)	4.30321 (-2)	1.06279 (-2)	2.12653 (-3)	2.59263 (-4)	1.68657 (-5)	4.53469 (-7)
1830 - 1840	49.1384	5.16936 (+1)	4.45972 (-2)	1.22676 (-2)	2.54289 (-3)	2.28142 (-4)	3.82202 (-6)	- 2.80316 (-7)
1840 - 1850	50.1323	5.24937 (+1)	3.90603 (-2)	1.11385 (-2)	2.54012 (-3)	2.60706 (-4)	9.28528 (-6)	—
1850 - 1860	50.2588	5.29072 (+1)	5.14423 (-2)	1.44397 (-2)	2.67736 (-3)	2.67504 (-4)	1.25948 (-5)	2.01172 (-7)
1860 - 1870	50.1323	5.28284 (+1)	4.49545 (-2)	1.27869 (-2)	3.02669 (-3)	3.72476 (-4)	2.06245 (-5)	3.98251 (-7)
1870 - 1880	51.7482	5.43478 (+1)	3.66791 (-2)	4.17660 (-3)	1.47417 (-4)	- 2.12345 (-6)	—	—
1880 - 1890	50.7790	5.36676 (+1)	4.53543 (-2)	1.03020 (-2)	1.83785 (-3)	1.68931 (-4)	5.68145 (-6)	—
1890 - 1900	52.3372	5.42884 (+1)	2.74950 (-2)	2.04873 (-3)	- 2.03154 (-4)	- 3.09675 (-5)	- 8.92868 (-7)	—
1900 - 1910	51.3230	5.42585 (+1)	4.48073 (-2)	9.45018 (-3)	1.70178 (-3)	1.84340 (-4)	9.38967 (-6)	1.65569 (-7)
1910 - 1920	52.3372	5.40122 (+1)	2.15554 (-2)	- 5.37363 (-4)	- 7.31229 (-4)	- 6.23199 (-5)	3.23266 (-8)	9.66567 (-8)
1920 - 1930	52.3372	5.50572 (+1)	2.85247 (-2)	4.17517 (-4)	- 2.50128 (-4)	- 1.40539 (-5)	- 5.24836 (-8)	—
1930 - 1940	52.3372	5.40083 (+1)	2.20002 (-2)	2.62723 (-5)	- 4.44432 (-4)	1.43133 (-6)	5.92530 (-6)	2.88189 (-7)
1940 - 1950	52.3372	5.39047 (+1)	1.87485 (-2)	6.27526 (-4)	- 9.40523 (-5)	- 3.01527 (-6)	1.73142 (-7)	—
1950 - 1960	52.3372	5.38956 (+1)	2.19236 (-2)	1.49760 (-3)	- 1.71685 (-4)	- 2.35142 (-5)	- 6.73216 (-7)	—
1960 - 1970	52.3372	5.35390 (+1)	1.86689 (-2)	3.28509 (-3)	4.49567 (-5)	- 2.01682 (-5)	- 8.56470 (-7)	—
1970 - 1980	52.3372	5.37112 (+1)	1.87544 (-2)	1.38674 (-3)	- 1.29624 (-4)	- 2.08988 (-5)	- 7.17849 (-7)	—
1980 - 1990	52.3372	5.33989 (+1)	1.43302 (-2)	2.93594 (-3)	2.02428 (-4)	3.54629 (-6)	—	—
1990 - 2000	52.3372	5.34105 (+1)	1.39964 (-2)	3.91794 (-3)	5.59879 (-4)	3.79849 (-5)	8.20535 (-7)	- 1.12618 (-8)
2000 - 2010	52.3372	5.33760 (+1)	1.26958 (-2)	2.61779 (-3)	1.71905 (-4)	- 6.65420 (-6)	- 1.24190 (-6)	- 4.01984 (-8)
2010 - 2020	52.3372	5.32539 (+1)	5.63802 (-3)	1.00563 (-3)	6.26682 (-5)	9.68210 (-7)	—	—
2020 - 2030	52.3372	5.33438 (+1)	9.34520 (-3)	3.02825 (-3)	4.79717 (-4)	3.61907 (-5)	1.03344 (-6)	—
2030 - 2040	52.3372	5.32898 (+1)	6.24672 (-3)	1.50722 (-3)	1.78772 (-4)	1.09906 (-5)	2.86579 (-7)	—
2040 - 2050	52.3372	5.32468 (+1)	3.39325 (-3)	4.03809 (-4)	8.51021 (-6)	- 5.21570 (-7)	—	—

* $(+1) = 10^{1}$; $(-1) = 10^{-1}$.

Table X.- Standard deviation for the 10 Å approximations $R^{*}_{\Delta\lambda}(M)$ and $R^{*}_{\Delta\lambda}(O_2)$

Interval (Å)	$s[R^{*}_{\Delta\lambda}(M)]$ (%)	$s[R^{*}_{\Delta\lambda}(O_2)]$ (%)	Interval (Å)	$s[R^{*}_{\Delta\lambda}(M)]$ (%)	$s[R^{*}_{\Delta\lambda}(O_2)]$ (%)
1750 - 1760	2.31	5.36	1900 - 1910	3.23	4.18
1760 - 1770	0.80	1.83	1910 - 1920	1.33	5.38
1770 - 1780	0.68	2.09	1920 - 1930	0.76	3.78
1780 - 1790	1.12	3.85	1930 - 1940	2.47	6.88
1790 - 1800	1.13	4.31	1940 - 1950	0.44	3.08
1800 - 1810	0.97	5.73	1950 - 1960	1.55	5.28
1810 - 1820	1.19	5.44	1960 - 1970	1.13	9.37
1820 - 1830	2.38	3.74	1970 - 1980	0.57	1.91
1830 - 1840	4.74	2.58	1980 - 1990	0.48	5.38
1840 - 1850	5.11	3.31	1990 - 2000	0.56	1.39
1850 - 1860	3.89	2.96	2000 - 2010	0.26	1.48
1860 - 1870	5.28	2.92	2010 - 2020	0.09	3.95
1870 - 1880	2.18	6.43	2020 - 2030	0.26	1.38
1880 - 1890	3.36	3.99	2030 - 2040	0.09	2.63
1890 - 1900	0.76	5.97	2040 - 2050	0.12	4.13

CONCLUSION

The penetration of solar radiation in the Schumann-Runge spectral range and the subsequent photodissociation of O_2 and minor constituents require lengthy computations when the detailed structure of the O_2 absorption cross section is taken into account. Since the resulting physical effect is important over a great height range from the lower thermosphere down to the stratosphere (see Figure 9), numerical approximations have been developed for a wide range of practical applications.

The introduction of reduction factors provides a simple technique for the calculation of the attenuation of solar radiation. Photodissociation of minor constituents is then easily computed when their absorption cross sections can be approximated by constant values over each interval (band, 500 cm^{-1}, 10 Å) in the Schumann-Runge spectral range. It is, however, necessary to average the solar flux available at the top of the atmosphere over each spectral interval covered by the reduction factors. This excludes, therefore, calculations of photodissociation of minor constituents with a rotational structure in their absorption cross sections as NO, for example (Cieslik and Nicolet, 1973).

Adoption of the analytical approximation given by expression (16) allows a direct computation of the reduction factors as a function of the O_2 total content. Since solar fluxes can be averaged over different intervals (band, 500 cm^{-1} or 10 A) the numerical coefficients required for the reduction factors have been computed for each type of interval over the Schumann-Runge spectral range (see Tables II, III, V, VI, VIII and IX). When a specific spectral interval is adopted, it is easy to develop a computer subroutine for the reduction factors. Such a subroutine requires the storage of 256, 320, or 480 coefficients when the adopted spectral interval is respectively 500 cm^{-1}, "band" or 10 Å. The total photodissociation coefficients are obtained by a simple summation over the spectral intervals of the Schumann-Runge system.

The same set of coefficients can be used for different solar zenith distances and for a wide range of atmospheric models. Furthermore, the numerical coefficients do not depend on the values adopted for the solar fluxes and for the average absorption coefficients of the minor constituents. Absorption by atmospheric ozone is easily taken into account through the factor $\exp[-\tau(O_3)]$ in expressions (13) to (15).

In summary, it appears that a simple procedure is now available for the analysis of absorption and photodissociation in the spectral range of the Schumann-Runge bands of molecular oxygen.

ACKNOWLEDGMENT

The author wishes to thank Prof. M. Nicolet for the constructive discussions during the preparation of this paper.

REFERENCES

ACKERMAN, M., Ultraviolet solar radiation related to mesospheric processes, in Mesospheric Models and Related Experiments (Ed. G. Fiocco), p. 149. Reidel, Dordrecht, Holland, 1971.

ACKERMAN, M., F. BIAUME and G. KOCKARTS, Absorption cross sections of the Schumann-Runge bands of molecular oxygen, *Planet. Space Sci.*, **18**,1639, 1970.

ALLISION, A.C., A. DALGARNO and N.W. PASACHOFF, Absorption by vibrationally excited molecular oxygen in the Schumann-Runge continuum, *Planet. Space Sci.*, **19**, 1463, 1971.

ANDERSON, J.G., Rocket-borne ultraviolet spectrometer measurement of OH resonance fluorescence with a diffusive transport model for mesospheric photochemistry, *J. Geophys. Res.*, 71. 4634, 1971.

BANKS, P.M. and G. KOCKARTS, *Aeronomy, Part A*, p. 182 Academic Press, New York, 1973.

BIAUME, F., Structure de rotation des bandes 0-0 à 13-0 du système de Schumann-Runge de l'oxygène moléculaire pp. 66, *Acad. Roy. Belg. Mém. Cl. Sci.*, **40**, 1972a.

BIAUME, F., Détermination de la valeur absolue de l'absorption dans les bandes du système de Schumann-Runge de l'oxygène moléculaire pp. 270, *Aeronomica Acta A* **100**, 1972b.

BIAUME, F., Nitric acid vapour absorption cross-section spectrum and its photodissociation in the stratosphere, *J. Photochem.*, 2, 139, 1973.

BRINKMANN, R.T., Dissociation of water vapor and evolution of oxygen in the terrestrial atmosphere, *J. Geophys. Res.*, 74, 5355, 1969.

BRINKMANN, R.T., Photochemistry and the escape efficiency of terrestrial hydrogen, in Mesospheric Models and Related Experiments (Ed. G. Fiocco), p.89, Reidel, Dordrecht, Holland, 1971.

CIESLIK, S. and M. NICOLET, The aeronomic dissociation of nitric oxide, *Planet. Space Sci.*, 21, 925, 1973.

COESA (Committee for the Extension to the Standard Atmosphere), The U.S. Standard Atmosphere, 1962, U.S. Government Printing Office, Washington, D.C., 1962.

COESA, The U.S. Standard Atmosphere Supplements, 1966, U.S. Government Printing Office, Washington, D.C., 1966.

CREEK, D.M. and R.W. NICHOLLS, A comprehensive re-analysis of the O_2 ($B\,^3\Sigma_u^- - X\,^3\Sigma_g^-$) Schumann-Runge band system, *Proc. R. Soc. Lond.* **A. 341**, 517, 1975.

FANG, T.-M., S.C. WOFSY and A. DALGARNO, Opacity distribution functions and absorption in Schumann-Runge bands of molecular oxygen, *Planet. Space Sci.*, **22**, 413, 1974.

HERZBERG, G., Molecular Spectra and Molecular Structure. I. Spectra of diatomic molecules 2nd ed. p. 122, Van Nostrand Reinhold, New York, 1950.

HUDSON, R.D. and S.H. MAHLE, Photodissociation rates of molecular oxygen in the mesosphere and lower thermosphere, *J. Geophys. Res.*, 77, 2902, 1972.

HUEBNER, R.H., R.J. CELOTTA, S.R. MIELCZAREK and C.E. KUYATT, Apparent oscillator strengths for molecular oxygen derived from electron - loss measurements, *J. Chem. Phys.*, **63**, 241, 1975.

JARMAIN, W.R. and R.W. NICHOLLS, A theoretical study of the v" = 0, 1, 2 progressions of bands and adjoining photodissociation continua of the O_2 Herzberg I system, *Proc. Phys. Soc.*, **90**, 545, 1967.

JULIENNE, P.S. and M. KRAUSS, Predissociation of the Schumann-Runge bands of O_2, *J. Mol. Spectrosc.*, **56**, 270, 1975.

KOCKARTS, G., Penetration of solar radiation in the Schumann-Runge bands of molecular oxygen, in Mesospheric Models and Related Experiments (Ed. G. Fiocco), p. 160, Reidel, Dordrecht, Holland, 1971.

KOCKARTS, G., Absorption par l'oxygène moléculaire dans les bandes de Schumann–Runge, *Aeronomica Acta A* 107, Fasc. I, 1972

NICOLET, M., Aeronomical reactions of hydrogen and ozone, in Mesospheric Models and Related Experiments (Ed. G. Fiocco), p. 1, Reidel, Dordrecht, Holland, 1971.

NICOLET, M., Atmospheric ozone : an introduction to its study, *Rev. Geophys. Sp. Phys.*, 13, 593, 1975.

NICOLET, M. and W. PEETERMANS, The production of nitric oxide in the stratosphere by oxidation of nitrous oxide, *Ann. Géophys.*, **28**, 751, 1972.

PARK, J.H., The equivalent mean absorption cross sections for the O_2 Schumann-Runge bands : application to the H_2O and NO photodissociation rates, *J. Atmos. Sci.*, **31**, 1893, 1974.

SAMAIN, D., R.M. BONNET, R. GAYET and C. LIZAMBERT, Stigmatic spectra of the sun between 1200 Å and 2100 Å, *Astron. Astrophys.*, **39**, 71, 1975.

SAMAIN, D. and P. SIMON, Solar flux determination in the spectral range 160-210 nm, *Solar Phys.*, 1976.

SHEMANSKY, D.E., CO_2 extinction coefficient 1700 - 3000 Å, *J. Chem. Phys.*, **56**, 1582, 1972.

SIMON, P., Extraterrestrial solar fluxes related to aeronomic processes, 1976.

WHITTEN, R.C. and R.P. TURCO, Perturbations of the stratosphere and mesosphere by aerospace vehicles, *AIAA J.*, **12**, 1110, 1974.

100 - BIAUME, F., Détermination de la valeur absolue de l'absorption dans les bandes du système de Schumann-Runge de l'oxygène moléculaire, 1972.

101 - NICOLET, M. and W. PEETERMANS, The production of nitric oxide in the stratosphere by oxidations of nitrous oxide, 1972.

102 - VAN HEMELRIJCK, E. et H. DEBEHOGNE, Observations au Portugal de phénomènes lumineux se rapportant à une expérience de lâcher de barium dans la magnétosphère, 1972.

103 - NICOLET, M. et W. PEETERMANS, On the vertical distribution of carbon monoxide and methane in the stratosphere, 1972.

104 - KOCKARTS, G., Heat balance and thermal conduction, 1972.

105 - ACKERMAN, M. and C. MULLER, Stratospheric methane from infrared spectra, 1972.

106 - ACKERMAN, M. and C. MULLER, Stratospheric nitrogen dioxide from infrared absorption spectra, 1972.

107 - KOCKARTS, G., Absorption par l'oxygène moléculaire dans les bandes de Schumann-Runge, 1972.

108 - LEMAIRE, J. et M. SCHERER, Comportements asymptotiques d'un modèle cinétique du vent solaire, 1972.

109 - LEMAIRE, J. and M. SCHERER, Plasma sheet particle precipitation : A kinetic model, 1972.

110 - BRASSEUR, G. and S. CIESLIK, On the behavior of nitrogen oxides in the stratosphere, 1972.

111 - ACKERMAN, M. and P. SIMON, Rocket measurement of solar fluxes at 1216 Å, 1450 Å and 1710 Å, 1972.

112 - CIESLIK, S. and M. NICOLET, The aeronomic dissociation of nitric oxide, 1973.

113 - BRASSEUR, G. and M. NICOLET, Chemospheric processes of nitric oxide in the mesosphere and stratosphere, 1973.

114 - CIESLIK, S. et C. MULLER, Absorption raie par raie dans la bande fondamentale infrarouge du monoxyde d'azote, 1973.

115 - LEMAIRE, J. and M. SCHERER, Kinetic models of the solar and polar winds, 1973.

116 - NICOLET, M., La biosphère au service de l'atmosphère, 1973.

117 - BIAUME, F., Nitric acid vapor absorption cross section spectrum and its photodissociation in the stratosphere, 1973.

118 - BRASSEUR, G., Chemical kinetic in the stratosphere, 1973.

119 - KOCKARTS, G., Helium in the terrestrial atmosphere, 1973.

120 - ACKERMAN, M., J.C. FONTANELLA, D. FRIMOUT, A. GIRARD, L. GRAMONT, N. LOUISNARD, C. MULLER and D. NEVEJANS, Recent stratospheric spectra of NO and NO_2, 1973.

121 - NICOLET, M., An overview of aeronomic processes in the stratosphere and mesosphere, 1973.

122 - LEMAIRE, J., The "Roche-Limit" of ionospheric plasma and the formation of the plasmapause, 1973.

123 - SIMON, P., Balloon measurements of solar fluxes between 1960 Å and 2300 Å, 1974.

124 - ARIJS, E., Effusion of ions through small holes, 1974.

125 - NICOLET, M., Aëronomie, 1974.

126 - SIMON, P., Observation de l'absorption du rayonnement ultraviolet solaire par ballons stratosphériques, 1974.

127 - VERCHEVAL, J., Contribution à l'étude de l'atmosphère terrestre supérieure à partir de l'analyse orbitale des satellites, 1973.

128 - LEMAIRE, J. and M. SCHERER, Exospheric models of the topside ionosphere, 1974.

129 - ACKERMAN, M., Stratospheric water vapor from high resolution infrared spectra, 1974.

130 - ROTH, M., Generalized invariant for a charged particle interacting with a linearly polarized hydromagnetic plane wave, 1974.

131 - BOLIN, R.C., D. FRIMOUT and C.F. LILLIE, Absolute flux measurements in the rocket ultraviolet, 1974.

132 - MAIGNAN, M. et C. MULLER, Méthodes de calcul de spectres stratosphériques d'absorption infrarouge, 1974.

133 - ACKERMAN, M., J.C. FONTANELLA, D. FRIMOUT, A. GIRARD, N. LOUISNARD and C. MULLER, Simultaneous measurements of NO and NO_2 in the stratosphere, 1974.

134 - NICOLET, M., On the production of nitric oxide by cosmic rays in the mesosphere and stratosphere, 1974.

135 - LEMAIRE, J. and M. SCHERER, Ionosphere-plasmasheet field aligned currents and parallel electric fields, 1974.

136 - ACKERMAN, M., P. SIMON, U. von ZAHN and U. LAUX, Simultaneous upper air composition measurements by means of UV monochromator and mass spectrometer, 1974.

137 - KOCKARTS, G., Neutral atmosphere modeling, 1974.

138 - BARLIER, F., P. BAUER, C. JAECK, G. THUILLIER and G. KOCKARTS, North-South asymmetries in the thermosphere during the last maximum of the solar cycle, 1974.

139 - ROTH, M., The effects of field aligned ionization models on the electron densities and total flux tubes contents deduced by the method of whistler analysis, 1974.

140 - DA MATA, L., La transition de l'homosphère à l'hétérosphère de l'atmosphère terrestre, 1974.

141 - LEMAIRE, J. and R.J. HOCH, Stable auroral red arcs and their importance for the physics of the plasmapause region, 1975.

142 - ACKERMAN, M., NO, NO_2 and HNO_3 below 35 km in the atmosphere, 1975.

143 - LEMAIRE, J., The mechanisms of formation of the plasmapause, 1975.

144 - SCIALOM, G., C. TAIEB and G. KOCKARTS, Daytime valley in the F1 region observed by incoherent scatter, 1975.

145 - SIMON, P., Nouvelles mesures de l'ultraviolet solaire dans la stratosphère, 1975.

146 - BRASSEUR, G. et M. BERTIN, Un modèle bi-dimensionnel de la stratosphère, 1975.

147 - LEMAIRE, J. et M. SCHERER, Contribution à l'étude des ions dans l'ionosphère polaire, 1975.

148 - DEBEHOGNE, H. et E. VAN HEMELRIJCK, Etude par étoiles-tests de la réduction des clichés pris au moyen de la caméra de triangulation IAS, 1975.

149 - DEBEHOGNE, H. et E. VAN HEMELRIJCK, Méthode des moindres carrés appliquée à la réduction des clichés astrométriques, 1975.

150 - DEBEHOGNE, H. et E. VAN HEMELRIJCK, Contribution au problème de l'abérration différentielle, 1975.

151 - MULLER, C. and A.J. SAUVAL, The CO fundamental bands in the solar spectrum, 1975.

152 - VERCHEVAL, J., Un effet géomagnétique dans la thermosphère moyenne, 1975.

153 - AMAYENC, P., D. ALCAYDE and G. KOCKARTS, Solar extreme ultraviolet heating and dynamical processes in the mid-latitude thermosphere, 1975.

154 - ARIJS, E. and D. NEVEJANS, A programmable control unit for a balloon borne quadrupole mass spectrometer, 1975.

155 - VERCHEVAL, J., Variations of exospheric temperature and atmospheric composition between 150 and 1100 km in relation to the semi-annual effect, 1975.

156 - NICOLET, M., Stratospheric Ozone : An introduction to its study, 1975.

157 - WEILL, G., J. CHRISTOPHE, C. LIPPENS, M. ACKERMAN and Y. SAHAI, Stratospheric balloon observations of the southern intertropical arc of airglow in the southern american aera, 1976.

158 - ACKERMAN, M., D. FRIMOUT, M. GOTTIGNIES, C. MULLER, Stratospheric HCl from infrared spectra, 1976.

159 - NICOLET, M., Conscience scientifique face à l'environnement atmosphérique, 1976.